Leptin and Insulin Sensitivity

by

John Joseph Dubé

BS, Shenandoah University, 1995

MS, James Madison University, 1997

Submitted to the Graduate Faculty of

Health and Physical Activity, in partial fulfillment

of the requirements for the degree of

Doctor of Philosophy

University of Pittsburgh

2005

UNIVERSITY OF PITTSBURGH

FACULTY OF HEALTH AND PHYSICAL ACTIVITY AND SCHOOL OF MEDICINE

This dissertation was presented

by

JOHN J. DUBÉ

It was defended on

April 8, 2005

and approved by

BRET GOODPASTER, PhD
Dissertation Director

FREDRIC L. GOSS, PhD

ADOLFO GARCIA-OCAÑA, PhD

ALLAN Z. ZHAO, PhD

LEPTIN AND INSULIN SENSITIVITY

JOHN J. DUBÉ, MS

University of Pittsburgh, 2005

Leptin-induced increases in skeletal muscle (SkM) insulin sensitivity (IS) are associated with decreases in SkM lipid levels (Buettner et al. *Am J Physiol*, 278: E563-E569,2000). However, the role of altered lipid metabolism in the beneficial effects of leptin on SkM IS is poorly understood. The current study addressed the effects of hyperleptinemia (HLEP) on acute hyperlipidemia-induced insulin resistance. Control (CONT) male Wistar rats were infused with either saline (CONT-SAL) or lipid (CONT-LIP) for 5h (5ml/kg/h) followed by a hyperinsulinemic-euglycemic clamp (15mU/kg/min insulin). Gucose infusion rates (GIR) were significantly lower in CONT-LIP vs. CONT-SAL (31.9±1.1 vs. 38.5±0.8 mg/kg/min, P=0.004, n=6/group). As previously reported the lipid metabolites diacylglycerol (DAG, 2.8±0.2 vs 2.1±0.3nMol/mg protein) and ceramide (CER, 0.8±0.1 vs 0.5±0.01nMol/mg protein) were elevated, and triglyceride (TG, 27.5±3.4 vs 41.0±5.7μg/mg protein) decreased (all P<0.05), in soleus muscle (SOL) in LIP vs SAL. In contrast to control animals a lipid infusion in HLEP (plasma leptin=57.8 ng/ml for 5 days) had no effect on GIR compared to saline-infused HLEP (43.0±4.1 vs. 43.8±5.1 mg/kg/min, P=0.40, n=6/group). Furthermore, DAG (2.8±0.2 vs 2.3±0.2), CER (1.1±0.1 vs 1.0±0.1), and TG (17.1±4.9 vs 16.0±2.6) levels in SOL were similar in HLEP-LIP and HLEP-SAL (all P>0.10). Fatty acid oxidation in the isolated SOL, acetyl CoA carboxylase phosphorylation (ACC-P), and the expression of the putative fatty acid transporters FAT/CD36 and FABPpm were similar in HLEP vs CONT. However, membrane-associated PKCθ was decreased in HLEP-LIP compared to CONT-LIP. We conclude that (1) HLEP prevents IR induced by a lipid infusion, (2) HLEP SkM does not accumulate DAG or CER or deplete TG in response to a lipid infusion, (3) altered FAox or FABP, FAT/CD36 expression are not likely sufficient to explain the effects of HLEP, and (4) membrane-associated PKCθ is suppressed following acute hyperlipidemia in hyperleptinemic animals.

TABLE OF CONTENTS

LIST OF FIGURES

LIST OF TABLES

I. Specific aims

Type 2 diabetes and obesity are now considered worldwide epidemics. Associated with these chronic diseases are hyperglycemia and hyperinsulinemia resulting from the development of insulin resistance (IR) at skeletal muscle (SkM) and liver. Major contributors to SkM IR include excessive dietary intake (i.e. lipid oversupply) (18, 30, 34), genetic predisposition (16), and lack of contractile or nervous system activity (49). It has been demonstrated that treatment with the adipocyte hormone leptin elicits decreases in SkM lipid content (7, 52) and improves insulin sensitivity (7, 11, 25, 51) in rodent models of IR possibly by lowering tissue and plasma lipids. However, there have been no studies that directly address the ability of leptin to prevent IR induced by lipid oversupply. In the current work, four specific address the mechanisms of leptin in the modulation of insulin sensitivity, particularly as they relate to altered lipid metabolism.

Specific aim 1. To confirm that exogenous lipid infusion elicits IR and evaluate alterations in SkM lipid species in various fiber types in the rat *in vivo*, in response to acute hyperlipidemia.

Specific aim 2. To determine if chronic hyperleptinemia prevents the development of IR caused by lipid oversupply *in vivo*.

Specific aim 3. To determine the mechanisms involved in the leptin-associated prevention of lipid induced insulin resistance at SkM.

Specific aim 4. To determine if chronic hyperleptinemia prevents the development of IR caused by hindlimb denervation.

II. Background and significance

A. Overview

Skeletal muscle insulin resistance is associated with a myriad of diseases including hypertension, coronary artery disease, and non-insulin dependant diabetes mellitus (NIDDM) or Type 2 diabetes. Type 2 diabetes accounts for over $100 billion in healthcare costs annually in the United States alone. It is estimated that while a majority of Type 2 diabetes cases are diagnosed in First World countries, as many as 8% of cases go undiagnosed in Third World countries (13). Because skeletal muscle (SkM) is the primary site for glucose disposal, understanding the mechanisms that contribute to the development of insulin resistance (IR) will lead to interventions that improve insulin action and thus a reduction in the prevalence of Type 2 diabetes and other related diseases.

B. Lipids and insulin resistance

While a number of factors contribute to the development of IR, several reports have implicated lipid oversupply as an essential player in the manifestation of IR (15, 18, 27). Specifically, accumulation of various lipid species including diacylglyceride (DAG) and ceramide leads to alterations in the insulin signaling pathway and subsequent decreases in insulin-stimulated glucose metabolism (31, 55). In a normal homeostatic model (i.e. energy supply equals energy demand), tissues in the body operate under a tight metabolic control. For example, the primary function of adipose tissue is storage of triglycerides (TG) and release of free fatty acids (FFA) for energy. A primary function of the liver is the *de novo* synthesis of FFA and export of lipids to adipose tissue and SkM in the form of lipoprotein complexes. Finally, pancreatic beta cells are designed to produce insulin during the fed state and alpha cells to secrete glucagon during the fasted state. In the face of energy oversupply,

however, these metabolically active tissues undergo metabolic changes that have deleterious consequences including excessive storage of TG in adipose tissue and subsequent increases in FFA release into circulation. Additionally, there is an increase in the *de novo* synthesis of FFA by the liver, further increasing levels of circulating plasma FFA. Consequently, there is an inappropriate storage of FFA in SkM and subsequent increase of insulin secretion in response to developing IR. Because SkM is the primary site for glucose disposal and a site for developing IR, the following review of literature will focus on alterations of SkM metabolism resulting from lipid oversupply by exogenous infusion and hindlimb denervation.

The development of elevated tissue lipid can be achieved through a variety of methods including excess dietary intake (40, 41), exogenous lipid infusion (31, 59), and denervation of SkM (55). Elevation of plasma FFA by exogenous TG lipid emulsion (i.e. lipid infusion or Intralipid) leads to the development of IR (15, 31, 44, 59) . This model has similar characteristics of elevated plasma FFA conditions observed in dietary induced IR animal models (34) and the development of IR occurs in a short time period (3-5 hours) (59). In humans, a 5h Intralipid infusion impairs insulin action at the whole body level independent of plasma glucose and insulin levels (15). Intralipid-induced IR, directly related to elevated plasma FFA levels brought on by the Intralipid infusion, elicits decreased rates of glucose oxidation and glycogen synthesis in SkM and impaired insulin signal transduction, at least at the level of phosphatidylinositol 3-kinase (PI3-kinase) activity. The authors speculate that FFA may affect glucose transport activity directly (i.e. down-regulation of GLUT-4 translocation to the cell membrane and subsequent decreases in glucose uptake) or could be the result of FFA-induced alterations in upstream signaling events. Studies in animal models of lipid-induced IR demonstrate very similar findings with regards to changes in whole body

insulin action and PI3-kinase activity (35, 59). In addition, other aspects of the insulin signaling cascade (IRS1 associated PI3-kinase, IRS1 phosphorylation and membrane associated protein kinase C (PKC) θ) respond to Intralipid infusion in a way that would predict impaired transduction of the insulin signal in SkM (24, 35). Taken together, these data demonstrate that the exogenous elevation of plasma FFA can elicit SkM IR and create deleterious alterations in the insulin-signaling pathway, specifically decreases in IRS-1 tyrosine phosphorylation and PI3-kinase activity.

Another model of IR that may involve alterations in lipid metabolism is hindlimb denervation. Insulin resistance in SkM following acute hindlimb denervation is the result of several complex mechanisms, many of which are currently unknown. It appears that biochemical and histological changes including increases in lipid content and decreases in glucose transporters are, in part, contributing to energy dysregulation. Denervation causes decreases in basal glucose uptake rates of approximately 49% (12, 56). This decrease in glucose uptake is a function of decreases in glucose transporters, including GLUT-4. While it has been reported that there are no differences in GLUT-4 levels 24-hous following denervation (17), there are significant decreases in GLUT-4 (69%) and GLUT-1 RNA (95%) levels 72-hours after denervation (8). There are several changes in mitochondria oxidative enzymes following denervation leading to a decrease in FFA used by the muscle. Further, there appears to be a "change" in fiber type following denervation. For example, oxidative muscles (i.e. soleus muscle) seem to become glycolytic due to decreases in oxidative enzymes (60).

Skeletal muscle lipid content is significantly altered as a result of denervation. Triglyceride content has been reported to decrease following 72 hours of denervation.

Further, reports indicate increases of approximately 30% of DAG following 72 hour denervation (55). The increase in DAG content following denervation may lead to increased PKC activation as evidenced by an increase in membrane-associated PKC (29). An increase in PKC activation can lead to a feedback inhibition of various components of insulin action (10). Finally, denervation has been shown to increase ceramide levels of approximately 34% (55) possibly leading to a repression of insulin signaling.

C. Lipid metabolites implicated in the development of insulin resistance

1. Triglycerides

Triglycerides are stored in SkM as a source of energy (46). Muscle biopsy studies indicate significant increases in SkM TG content from both obese and Type 2 diabetic subjects (21). As such, it has been hypothesized that increased levels of intramyocellular TG (imTG) leads to the development of IR. However, increased levels of imTG, similar to those found in obese and Type 2 diabetics, have been reported in endurance-trained athletes (22). Thus, it appears that imTG may serve only as a marker for the development of IR. The mechanisms linking increased levels of intra-tissue TG and IR most likely revolve around the function of TG as a surrogate marker for the level of other lipid species, specifically, DAG and long-chain acyl CoAs (LCACoAs) and ceramide (20).

2. Diacylglycerides

Diacylglycerides serve as substrates for other lipids including TG and monoacylglycerides and are increased in various models of SkM IR including exogenous lipid infusion (31, 59) and denervation (55). Recently, time course studies investigating the alterations in SkM lipid species content following the infusion of a lipid emulsion have been reported in rodents (59). As expected, Intralipid infusion elicites significant (~3-4 fold)

increases in DAG content of soleus (SOL) muscle; a muscle composed predominately of slow, oxidative fibers that are highly insulin sensitive. However, the significant accumulation of DAG content peaks at 3-4h and returns to baseline values at 5h. These data demonstrate that SkM lipid content, specifically DAG, is increased during a Intralipid infusion and the elevation of intramyocellular lipid in rodents is somehow corrected, but the deleterious effects on insulin action remain (24). Human biopsy studies have demonstrated similar elevations SkM DAG (~3 fold) content following Intralipid infusion (3, 31). Finally, increases in SkM DAG content have been observed in the hindlimb denervation model of IR (55). Taken together, these data support the hypothesis of elevated DAG content in SkM as a potential mediator of IR.

3. Ceramides

Sphingolipids are one of the major phospholipids in cell membranes (23) and serve an important role in the signal transduction process. The hydrolysis of sphingomyelin produces ceramide, a second messenger, within the cell. In addition, ceramides can be formed *de novo* from serine and palmitoyl-CoA (47). Ceramides are present in SkM and are involved in cell differentiation, inhibition of cell proliferation, regulation of inflammatory processes, and induction of apoptosis (23). Additionally, ceramides may play a role in the regulation of glucose uptake in SkM (53). In denervated SOL muscle, ceramide content is elevated ~40%, comparable to the observed elevation of DAG (55), however, it appears that acute lipid oversupply (Intralipid) may not elicit the same increase in ceramides (31, 59).

As stated previously, ceramide may be important regulator of glucose uptake (14, 48, 53, 55) in SkM. In C2C12 cells pretreated with palmitate (48), insulin-stimulated glucose uptake and glycogen synthesis are significantly decreased (~20%) coinciding with a 100% higher

ceramide content compared to controls. Human biopsy studies (1) indicate insulin-resistant obese subjects have significantly higher basal levels of total ceramide compared to insulin-sensitive lean controls. However, insulin stimulation elicits similar increases in total and individual ceramides in insulin-resistant and insulin-sensitive subjects. Taken together these data demonstrate that the accumulation of SkM ceramide is associated IR, but that in the presence of insulin, SkM ceramide content is elevated regardless of the degree of insulin sensitivity.

D. Mechanisms of insulin resistance induced by lipid oversupply

The accumulation of SkM lipid content is associated with the development of IR. In addition, IR is associated with decreases in SkM fatty acid oxidation, increases in fatty acid transport, and activation of membrane-associated PKCθ leading to deleterious effects on the insulin-signaling pathway. However, mechanisms contributing to IR appear to be independent of decreases in FAox.

Acute high-fat feeding (~4 days) has been demonstrated to increase the expression of malonyl-CoA decorboxylase (MCD) in rat SkM (soleus) demonstrating that the initial response to increased substrate availability is increased FAox. However, in several human models of IR (i.e. obesity and diabetes) decreased levels of FAox are observed (32) in conjunction with increased levels of SkM lipid content. Further, infusion of Intralipid has been demonstrated to significantly increase fatty acid transport into rat SkM (57). Therefore, while the initial response to lipid oversupply is increased FAox, the increase in SkM lipid content leads to the inappropriate storage and accumulation of lipids, specifically DAG and ceramide. The accumulation of these lipid species leads to deleterious effects on the insulin-signaling pathway.

The accumulation of ceramide in C2C12 myoblasts elicits decreases in insulin-stimulated phosphorylated Akt/PKB (phospho Akt/PKB) and glycogen synthase kinase-3 (GSK-3) activity (48). However, it is interesting to note that several upstream targets of the insulin-signaling cascade are unaffected by the preincubation of FFA including IRS-1 phosphorylation and PI3-kinase activity. In insulin-resistant obese human subjects, ceramide content is twice that of normal controls. Additionally, insulin stimulation elicits a significant decrease in Akt phosphorylation (1). Taken together these data suggest that the elevation of ceramides alter the insulin-signaling pathway at levels independent of IRS-1 phosphorylation and PI3-kinase activity. Moreover, these data infer that the decrease Akt/PKB phosphorylation by ceramides may lead to decreases in GLUT-4 translocation as demonstrated by observed decreases in glucose uptake.

Finally, increases in SkM DAG are associated with the development of IR (24, 31), specifically by altering the insulin-signaling pathway (Review in (47)). The principle mechanism by which DAG alters insulin signaling is through the activation of membrane-associated PKCθ (24, 59). Time-course studies (59) indicate that following a 5h lipid infusion, total SkM PKCθ levels appear to decrease, however, membrane-associated PKCθ levels are significantly increased. Increases in membrane-associated PKCθ are correlated with increased levels of IRS-1 serine phosphorylation and decreased levels of IRS-1 tyrosine-associated PI3-kinase activity (59), leading to subsequent decreases in glucose uptake.

Taken together the data demonstrate that an increase in substrate availability (i.e. lipid oversupply) to SkM elicits an initial increase in FAox. However, subsequent increases in fatty acid transport into SkM lead to inappropriate storage of lipids such as DAG and ceramide. This inappropriate storage activates several second messenger systems that act to

disrupt the insulin-signaling pathway leading to the development of IR. Fig. 1 summarizes the associated between lipid oversupply and the development of IR.

E. Leptin

The adipocyte-derived hormone leptin is an important regulator of energy intake and metabolism. In 1959, Hervey demonstrated that cross-circulation between rats rendered obese by hypothalamic lesions and control rats leads to starvation in the controls (28). The inhibition of food intake was initially attributed to an unknown circulating satiety factor. Further, obese rats are unable to respond to this factor due to the hypothalamic lesion. Additional studies using the diabetic and insulin resistant mutation-rodent model *ob/ob* mouse, which lacks leptin and is obese, demonstrate that the administration of leptin elicits decreases in food intake and increases in energy expenditure (26). As such, leptin was first thought to be an anti-obesity hormone. However, subsequent work has provided insights into the complex role of leptin in energy regulation.

It is now clear that leptin can improve glucose metabolism (7, 11, 39). In rodents, diet-induced lipid oversupply decreases insulin-stimulated 2-deoxyglucose (2-DG) uptake and increases SkM TG content (7). Leptin treatment restores SkM 2-DG uptake and decreases TG content in fat fed rats to levels of lean controls. Studies from other diabetic rodent models including *ob/ob* (39) and streptozotocin-induced diabetic mice (11), demonstrate that leptin treatment lowers fasting insulin and glucose levels, and improves glucose metabolism compared to normal controls. In addition to improvements in glucose uptake, leptin administration has been demonstrated to restore glucose transporter levels (GLUT-4) to those of controls in high-fat fed rats (58). Finally, leptin administration elicits a significant

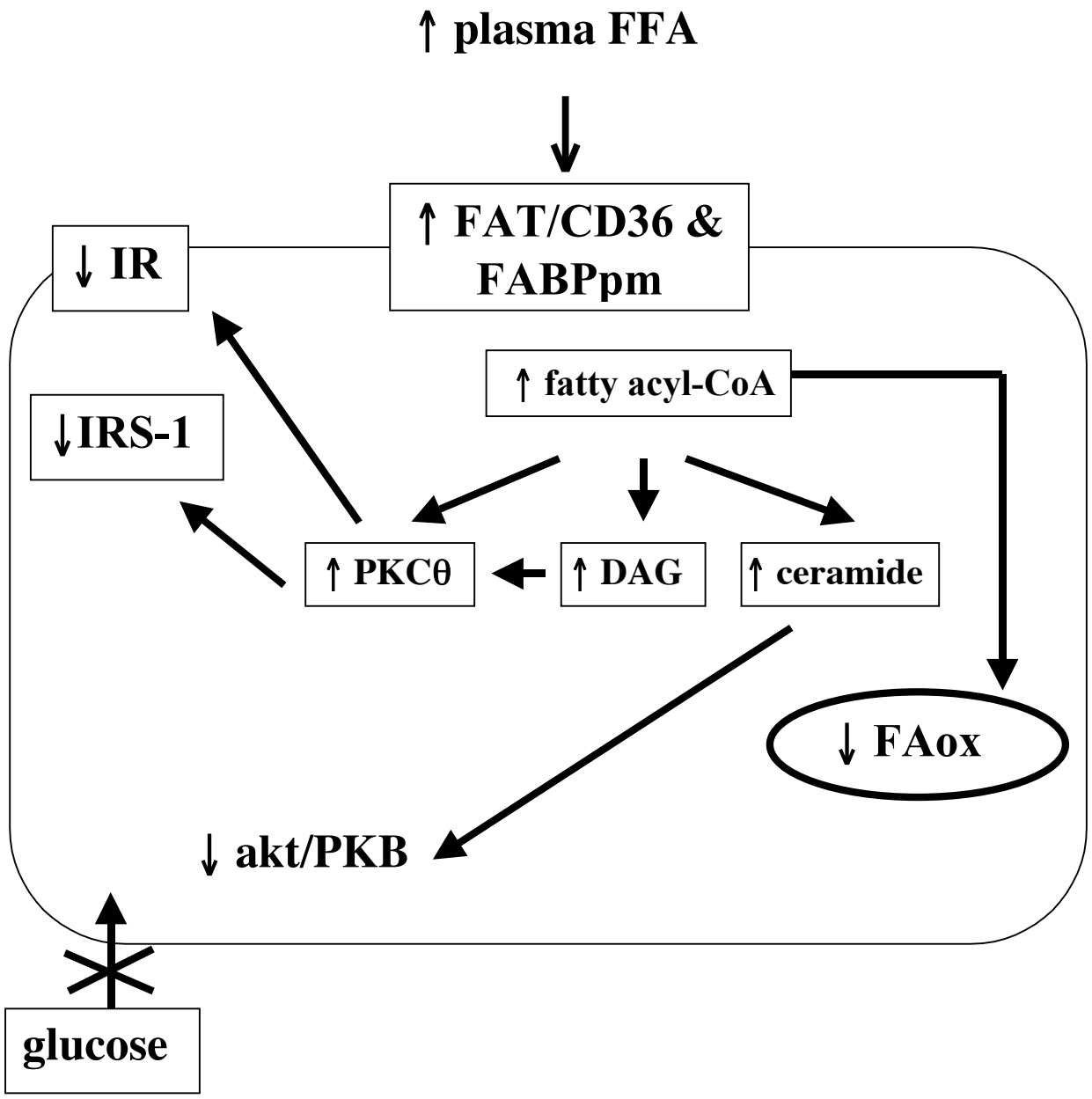

Fig. 1. ***Summary of lipid accumulation and development of IR.*** **Lipid oversupply in the form of high-fat feeding or Intralipid leads to elevated levels of plasma FFA. There is a subsequent upregulation of fatty acid transport into SkM leading to increased levels of fatty acyl-CoA and inappropriate storage of various lipid species including DAG and ceramide. The accumulation of fatty acyl-CoA leads to subsequent decreases in fatty acid oxidation (FAox). As lipids accumulate, they begin to act as second messengers leading to the development of IR. While, PKCθ is activated by DAG and elicits deleterious effects on the insulin signaling cascade, ceramide downregulates akt/PKB activity decreasing glucose uptake.**

decrease of FA incorporated into TG in isolated SOL muscles from *ob/ob* mice following incubation with leptin. These data demonstrate the role of leptin in glucose uptake and an alteration in lipid partitioning by leptin (37).

Leptin has been demonstrated to induce significant improvements in SkM lipid metabolism, specifically by increasing fatty acid oxidation, altering lipid partitioning, decreasing lipid content, and decreasing fatty acid transporters. However, reports remain controversial. In rats, chronic subcutaneous infusions does not improve exogenous palmitate oxidation or uptake in the basal state in isolated SkM (52). However, when muscles are stimulated to contract, exogenous palmitate oxidation is significantly increased in the leptin treated muscle compared to controls. The authors (52) speculated that it is necessary to increase the metabolic rate of SkM to detect alterations in FA metabolism from isolated SkM. However, a similar study using *ob/ob* mice demonstrated significant increases in FA oxidation in isolated SOL incubated in the presence of leptin when compared to controls without the need for SkM contraction (37). The fundamental difference between the FAox from isolated muscle studies is that SkM from *ob/ob* mice never "see" leptin, whereas "normal" rat SkM has been exposed to leptin. Therefore, it is reasonable to suggest that previous exposure to leptin will inhibit observable *ex vivo* metabolic responses. In contrast, SkM exposed to leptin for the first time *ex vivo* will respond appropriately. Finally, chronic leptin treatment (2-week subcutaneous infusion) in rats decreases fatty acid translocase (FAT/CD36) whole muscle and plasma protein expression in SOL muscles (51). Taken together these data demonstrate that leptin can regulate lipid metabolism by either a central mechanism, decreasing FAT/CD36 and FABPpm, or by a peripheral mechanism, direct exposure to exogenous leptin. While these results are encouraging with respect to a

treatment for SkM IR, FA oxidation has not been improved in obese humans with the administration of leptin suggesting the development of "leptin resistance" (52).

Leptin has been used as a treatment for lipodystrophy (2, 42), a disorder that is characterized by an abnormal loss of subcutaneous adipose tissue. Additionally, lipodystrophy is associated with hyperlipidemia, hepatic steatosis, and hyperglycemia resulting in the development of IR. Human and rodent studies demonstrate that the administration of leptin elicits a significant decrease in circulating FFA, normalizes plasma glucose levels, decreases intramyocellular lipid content, and reverses hepatic steatosis. These studies provide additional evidence of the complex role of leptin as it relates to insulin sensitivity and SkM lipid metabolism.

In summary, leptin has been demonstrated to be an important regulator of energy intake and insulin sensitivity. Several human and rodent models of IR including lipodystrophy, genetic mutations, and lipid oversupply have been used to establish leptin as a treatment method for the reversal of IR. The putative mechanisms associated with improvements on insulin action by leptin include decreased SkM lipid content, increased SkM FAox, and alterations in FAox gene expression. However, questions remain regarding the ability of leptin to prevent IR and maintain insulin sensitivity in spite of a known IR insult, specifically acute hyperlipidemia.

III. Methods

A. Models

Male Wistar rats (Charles River Laboratories, Wilmington, MA) weighing between 200-280 g were used for all experiments. Rats were individually housed in environmentally controlled conditions on a 12-h light-12-h dark cycle, fed a standard chow *ad libitum* with

free access to water, and acclimatized for 3-5 days prior to all experimental procedures. For all hyperinsulinemic-euglycemic clamp studies, the jugular vein and carotid artery were chronically cannulated in all animals. However, for all other infusion studies, only the carotid artery was chronically cannulated. Briefly, rats were anesthetized with ~250 μL of anesthesia mix containing 50mg/mL Ketamine, 5mg/mL Xylazine, and 1mg/mL Acepromazine. Using a sterile technique, the dorsal and ventral neck of the animals was shaved and scrubbed with Betadine. The skin was cut just superior to the sternal notch and the vessels exposed by blunt dissection. The cannula (PE50, Becton Dickinson, Sparks, MD) was cut to the desired length, inserted into the vessel and secured. A small incision was made on the dorsal side, midline, just caudal to the ears. A large blunt needle (10 GA) was inserted in the subcutaneous space and thread around to the ventral opening. The catheter was fed through the subcutaneous canal and out the dorsal incision. The cannula was filled with a 3:1 glycerol:heparinized saline (20 U/mL) and capped using a metal post. Following surgery, rats were allowed to recover until they reached preoperavtive weight (~5-7 days). All procedures were approved by the University of Pittsburgh Department of Laboratory Animals Research and Institutional Animal Care and Use Committee.

B. Experimental design

1. Lipid induced insulin resistance

Specific aim 1 was designed to address (1) Intralipid induces IR and (2) that mechanisms associated with the development of IR included increased accumulation of SkM lipids (i.e. DAG and ceramide). These studies were necessary to establish the framework for observations related to leptin treatment. Three groups of male Wistar rats were used for the following experiments.

The first group of rats was catheterized in the carotid artery and jugular vein as previously described and assigned to either a saline (SAL, n=6) or Intralipid (LIP, n=6) protocol. Rats were fasted overnight and procedures begun between 0700-0900h. The infusion and clamp protocol is summarized in Fig. 2. Briefly, plasma FFA concentrations were increased in conscious male Wistar rats by a 5h intravenous infusion of LIP (5 mL/kg/h, Liposyn II, Abbott Laboratories, North Chicago, Illinois) combined with a continuous infusion of heparin (6 U/h) to activate lipoprotein lipase. Control rats were infused with SAL (5 mL/kg/h) for 5h. Following the 5h infusion period, a 90-minute hyperinsulinemic (15 mU/kg/min)-euglycemic clamp was conducted using a variable 30% glucose infusion. It is important to note that the SAL or LIP solution continued throughout the clamp. Humulin regular insulin (Eli Lilly, Indianapolis, Indiana) was used during the clamps. Blood samples were taken every 5-10 minutes during the clamps to assess rates of glucose disposal. Approximately 50 μL of whole blood was centrifuged and plasma glucose determined using a Beckman Glucose Analyzer 2 (Beckman Instruments, Brea, CA). At the end of the clamp, a final blood sample (~300 μL) was taken for additional plasma analyses. The animals were then anesthetized with an intravenous injection of ~70mg/kg Nembutol, tissues quickly excised, and frozen in liquid nitrogen for later analysis. Glucose infusion rates were averaged the last 60-min of the clamp and used to assess of insulin sensitivity.

2. Lipid accumulation in skeletal muscle

The second and third groups of rats were used to examine increases in SkM lipid content resulting from Intralipid. Rats were catheterized in the carotid artery as previously described and assigned to one of four infusion conditions: (1) 3h SAL, (2) 3h LIP, (3) 6h SAL, or (4) 6h LIP. These infusion times were chosen based on (1) observations by Yu and colleagues

who observed significant increases in SkM DAG content following a 3h Intralipid infusion and (2) the total SAL or LIP infusion period of 5h infusion/clamp studies (~6.5 h). The summary of the infusion protocol is summarized in Fig. 3. Briefly, 18h overnight fasted conscious rats were infused with either SAL or LIP (5 mL/kg/h) for 3- or 6h. Following the infusion period, the animals were anesthetized with an intravenous injection of ~70mg/kg Nembutal, tissues quickly excised, and frozen in liquid nitrogen for later analysis.

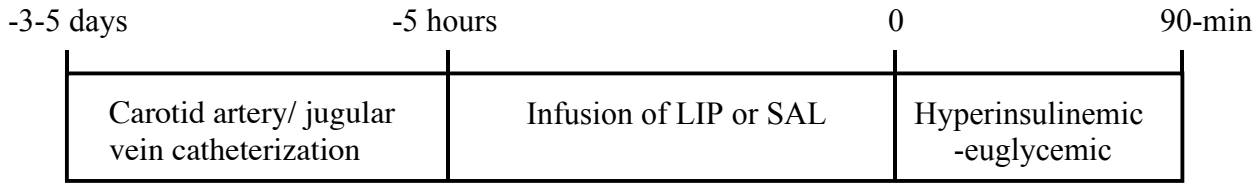

Fig. 2. ***Intralipid induced insulin resistance protocol.*** **Male Wistar rats were catheterized in the carotid artery and jugular vein 3-5 days prior to infusion and clamp studies. Plasma FFA concentrations were increased by a 5h intravenous infusion of Intralipid (LIP, 5 mL/kg/h, n=6) combined with a continuous infusion of heparin (6 U/h). Control rats were infused with saline (SAL, 5 mL/kg/h, n=6) for 5h. Following the 5h infusion period, a 90-minute hyperinsulinemic (15 mU/kg/min)-euglycemic clamp was conducted using a variable 30% glucose infusion. Blood samples were taken every 5 -10 minutes during the clamps to assess rates of glucose disposal. At the end of the clamp, a final blood sample was taken for additional plasma analyses. The animals were then anesthetized, tissues quickly excised, and frozen in liquid nitrogen for later analysis. Glucose infusion rates were averaged the last 60-min of the clamp and used to assess of insulin sensitivity.**

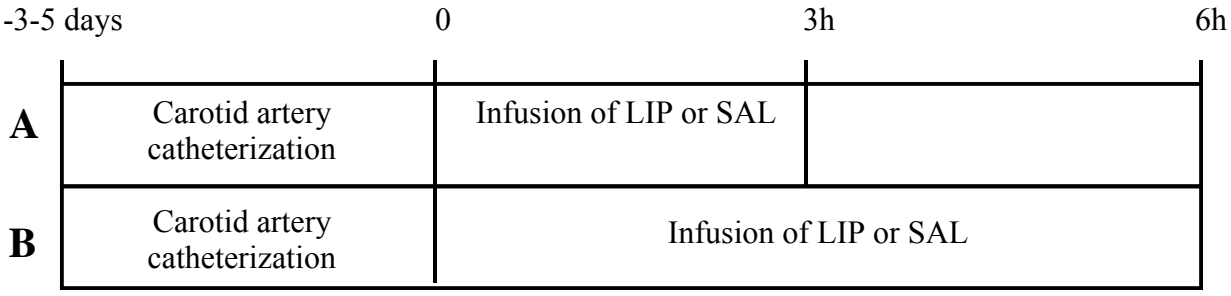

Fig. 3. ***3h and 6h Intralipid infusion protocol for analysis of SkM lipid.*** **Rats were catheterized in the carotid artery 3-5 days prior to all experiments. Plasma FFA concentrations were increased by an intravenous infusion of Intralipid (5 mL/kg/h) combined with a continuous infusion of heparin (6 U/h) for either 3h (Panel *A*) or 6h (Panel *B*). Control rats were infused with saline (5 mL/kg/h). Following the infusion period, the animals were anesthetized with ~70mg/kg Nembutal, tissues quickly excised, and frozen in liquid nitrogen for later analysis.**

3. Leptin effects on lipid induced insulin resistance

The following study addressed the ability of leptin treatment to prevent IR induced by Intralipid. Purified leptin virus was administered to conscious male Wister rats that were catheterized in the carotid artery and jugular vein as previously described. The principle site of expression of adenoviral vectors is the liver (>95%), with minor expression in the lung. Vectors are not expressed in other tissues (skeletal muscle, brain, pancreas, heart, kidney, adipose tissue). The length of expression is commonly 2 weeks or greater. Virus administration procedures were as follows. Rats were minimally restrained and the carotid artery cannula cleared with ~200 μL of heparinized saline. An IV injection of $1x10^{12}$ virus particles (leptin) in 300-350 μL of saline was slowly administered and followed by ~200 μL of saline. The cannula was filled with 3:1 glycerol:heparinized saline (20 U/mL) and capped using a metal post. Food intake and body weight were monitored for 5 days and rats were

randomly assigned to either a SAL (n=6) or LIP (n=6) protocol. Elevation of plasma FFA concentrations (5h infusion) and clamp procedures were completed as previously described. At the end of the clamp, a final blood sample was taken for additional plasma analyses. The animals were then anesthetized with an IV injection of ~70mg/kg Nembutal, tissues quickly excised, and frozen in liquid nitrogen for later analysis. Glucose infusion rates were averaged the last 60-min of the clamp and used to assess of insulin sensitivity. The experimental design for the leptin effects on lipid induced IR is summarized in Fig. 4.

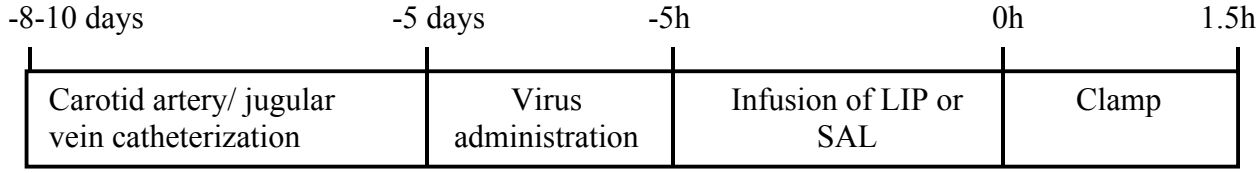

Fig. 4. ***Prevention of Intralipid induced insulin resistance by leptin protocol.*** **Rats were catheterized in the carotid artery and jugular vein. Following recovery to presurgical body weight, rats were rendered hyperleptinemic by the administration of an adenovirus containing rat leptin cDNA and assigned to either a Intralipid (LIP, n=6) or saline (SAL, n=6) infusion protocol. Food intake and body weight were monitored for 5d. Following an overnight fast, plasma FFA concentrations were increased by a 5h intravenous infusion of LIP (5 mL/kg/h, n=6) combined with a continuous infusion of heparin (6 U/h). Control rats were infused with SAL (5 mL/kg/h, n=6) for 5h. Following the 5h infusion period, a 90-minute hyperinsulinemic (15 mU/kg/min)-euglycemic clamp was conducted using a variable 30% glucose infusion. It is important to note that the SAL or LIP solution continued throughout the clamp. Humulin regular insulin (Eli Lilly, Indianapolis, Indiana) was used during the clamps. Blood samples were taken every 5 -10 minutes during the clamps to assess rates of glucose disposal. At the end of the clamp, a final blood sample was taken for additional plasma analyses. The animals were then anesthetized through an IV injection of ~70 mg/kg Nembutal, tissues quickly excised, and frozen in liquid nitrogen for later analysis. Glucose infusion rates were averaged the last 60-min of the clamp and used to assess insulin sensitivity.**

4. Leptin effects on skeletal muscle lipid accumulation

The next sets of studies were designed to address the mechanisms associated with lipid metabolism and improvements of insulin action mediated by leptin. Alterations in SkM lipid content (i.e. DAG, ceramide, and TG) were assessed in hyperleptinemic (HLEP) rats following 3h Intralipid. Procedures are summarized in Fig. 5. Briefly, male Wistar rats were chronically cannulated in the carotid artery as previously described. Following recovery to presurgical body weight, rats were rendered HLEP by the administration of leptin adenovirus and assigned to either a 3h SAL (n=6) or LIP (n=6) infusion protocol. Body weight and food intake were monitored for 5d. Rats were fasted overnight and plasma FFA concentrations elevated. Following the infusion period, the animals were anesthetized with an IV injection of ~70mg/kg Nembutal, tissues quickly excised, and frozen in liquid nitrogen for later analysis. SkM lipid content was assessed as previously described.

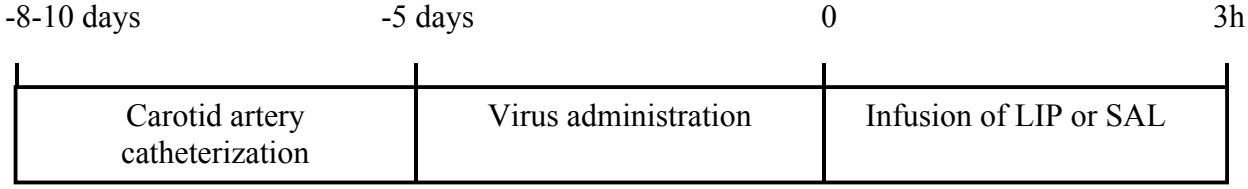

Fig. 5. ***3h Intralipid infusion following leptin treatment protocol.*** **Rats were catheterized in the carotid artery and following recovery of presurgical bodyweight rendered hyperleptinemic by adenovirus administration. Bodyweight and food intake were monitored for 5d and rats were randomly assigned to either a 3h saline (SAL, n=6) or Intralipid (LIP, n=6) infusion protocol. Plasma FFA concentrations were increased by an intravenous infusion of (5 mL/kg/h) combined with a continuous infusion of heparin (6 U/h) for 3h. Control rats were infused with saline (5 mL/kg/h) for 3h. Following the infusion period, the animals were anesthetized with an IV injection of ~70mg/kg Nembutal, tissues quickly excised, and frozen in liquid nitrogen for later analysis.**

5. Leptin effects on skeletal muscle fatty acid oxidation

The subsequent set of experiments addressed the affects of leptin treatment on FAox in isolated SOL muscles. A group of male Wistar rats (n=3) was rendered HLEP through a tail vein administration of adenovirus containing rat cDNA leptin. Briefly, rats were anesthetized under isoflurane and remained unconscious through an isoflurane saturated gauze pad placed just beyond the nose. The tail was shaved and sterilized using alcohol prep pads. A 24 GA 0.7 x 19mm catheter was carefully inserted into the lateral tail vein and flushed with saline. Saline containing 1 x 10^{12} particles/mL of leptin adenovirus (total volume ~400 μL) was slowly infused. The catheter was slowly removed and bleeding inhibited by pressure. Control rats (n=3) received no virus treatment, however, were calorically matched to leptin. Rats were monitored for food intake and body weight changes for 5d. Following an overnight fast, rats were anesthetized under isoflurane, SOL muscles quickly excised, and FAox measured as described below.

A second set of rats was used to examine P-ACC an allosteric regulator of FAox. Procedures are summarized in Fig. 5. Male Wistar rats were catheterized in the carotid artery and administered an adenovirus containing either leptin cDNA or βGal cDNA. Food intake and body weight changes were monitored for 5 days; βGals were calorically matched to leptin. Following an overnight fast, rats were infused for 3h with either saline or Intralipid. Immediately after the infusions, rats were anesthetized with ~70mg/kg Nembutal, tissues quickly excised, and frozen in liquid nitrogen for later analysis. Measurement of P-ACC is described below.

6. Leptin effects on fatty acid transporters

The examination of fatty acid transporter (FAT/CD36) and plasma membrane fatty acid binding protein (FABPpm) was kindly completed by Dr. Arend Bonen at the University of Guelph, Ontario, Canada. FAT/CD36 and FABPpm were assessed in GAS from 3h saline infused HLEP and βGal rats used for analysis of P-ACC as described above. Protein content was assessed by Western blot as described below.

7. Leptin effects on gene expression

Several metabolic genes were examined in SOL from 3h saline infused HLEP and βGal rats used for analysis of P-ACC as described above. Gene expression was assessed by RT-PCR as described below.

8. Leptin effects on PKCθ

The final set of studies examining the mechanisms associated with improvements in insulin action modulated by leptin addressed the activation of PKCθ. Specifically SOL muscle membrane and cytosolic fractions of PKCθ from HLEP and βGal 6h LIP infused animals were used. Briefly, male Wistar rats were catheterized in the carotid artery as previously described. Following a recovery to presurgical body weight, rats were administered adenovirus through the cannula containing either βGal or leptin. Leptin treated animals were monitored for body weight changes and food intake, βGals were pair-fed to leptin animals. Plasma FFA was elevated in leptin and βGal treated animals through a 6h Intralipid infusion as previously described. Following the infusion period, animals were anesthetized, tissues quickly excised, and frozen in liquid nitrogen for later analysis. To address the affect of leptin on PKCθ basal expression, a subsequent experiment examined

PKCθ fractions in HLEP and βGal treated animals that received no infusion. A summary of the PKCθ fractionation studies is found in Fig. 5.

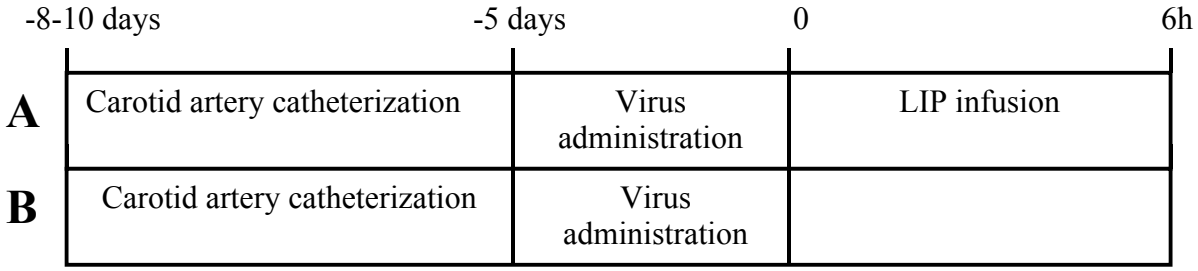

Fig. 6. ***PKCθ fraction studies protocol.*** **Male Wistar rats were catheterized in the carotid artery, allowed to recover to presurgical body weight, and administered an adenovirus through the cannula containing either βGal (n=6) or leptin (n=6). Leptin treated animals were monitored for body weight changes and food intake, βGals were pair-fed to leptin animals. In panel *A*, plasma FFA was elevated in leptin and βGal treated animals through a 6h Intralipid infusion as previously described. Following the infusion period, animals were anesthetized, tissues quickly excised, and frozen in liquid nitrogen for later analysis. The protocol in panel *B* addressed the affect of leptin on PKCθ fraction basal expression in HLEP (n=3) and βGal (n=3) treated animals. Male Wistar rats were catheterized in the carotid artery, allowed to recover to presurgical body weight, and sacrificed without infusions.**

9. Leptin effects on denervation induced insulin resistance

The following studies addressed leptin effects of lipid accumulation and the effects of insulin sensitivity in denervated skeletal muscle. To confirm IR following denervation, male Wistar rats were used in all experiments. Rats were individually housed in a controlled environment with a 12-h light-dark cycle, fed a standard chow *ad libitum*, and acclimatized for 3-5 days prior to experimental procedures. All surgical procedures were performed under isoflurane anesthesia. The left hindlimb of each rat was denervated. The sciatic nerve was exposed through a 1 to 2 cm incision on the lateral surface and blunt dissection of the thigh muscles. A 5-mm segment of the sciatic nerve was excised. The incision was closed with a 4-0-nylon suture. Because several reports demonstrate that contralateral sham operations do not effect the parameters changed by denervation, this procedure was not used.

Subsequent experiments were designed to examine the effect of leptin treatment on the prevention of IR by hindlimb denervation. Rats were administered an adenovirus containing either βGal or leptin through tail vein injection as described in Methods. Rats were monitored for food intake and body weight changed for 48h; βGals were calorically matched to leptin. After the initial 48h period, denervation procedures were completed as described in Methods. Rats were monitored for an additionally 72h for food intake and body weight changes. Following an overnight fast, rats were anesthetized under isoflurane, soleus muscles quickly excised and glucose uptake measured. The adenovirus/denervation protocol is summarized in Fig. 7.

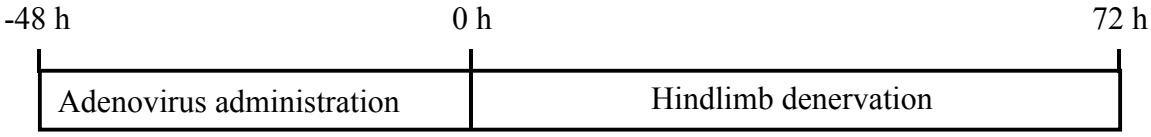

Fig. 7. ***Adenovirus and denervation protocol.*** **Male Wistar rats were administered an adenovirus containing either β-Galactosidase or leptin through tail vein injections as described in Methods. 48H later, the sciatic nerve was exposed and excised. Rats were monitored for 72h for food intake and body weight changes. Following an overnight fast, rats were anesthetized, soleus muscle quickly excised and glucose uptake measured.**

C. Tissue and plasma analysis

1. Measurement of skeletal muscle lipid content

For analysis of lipid species (i.e. DAG, ceramide, and TG) tissues were crushed while under liquid nitrogen and homogenized in ice-cold (80%) methanol (MeOH)/H_2O containing butylated-hydroxytoluene (5μg/mL) as an antioxidant. The MeOH/H_2O homogenate was mixed with chloroform ($CHCl_3$) (2:1 v/v $CHCl_3$:MeOH) to extract lipids as described by Folch *et al. (19)*. Briefly, the sample was homogenized 2 x 10 *s* and ~1.5 mL methanol was added (as compensation for the water added to the initial methanol mixture) to bring the sample to a single phase. Samples were centrifuged at 3,000 rpm for 30 minutes to spin down protein pellet. The supernatant was removed without disturbing the protein pellet and 0.2 volumes of 0.1 N sodium chloride (NaCl) added. The solution was vortexed for 30 seconds and centrifuged at 1500 rpm for 10 minutes. The bottom lipid-containing layer was removed, evaporated using a speed vacuum and stored at -80°C. Procedures are summarized in Fig. 8.

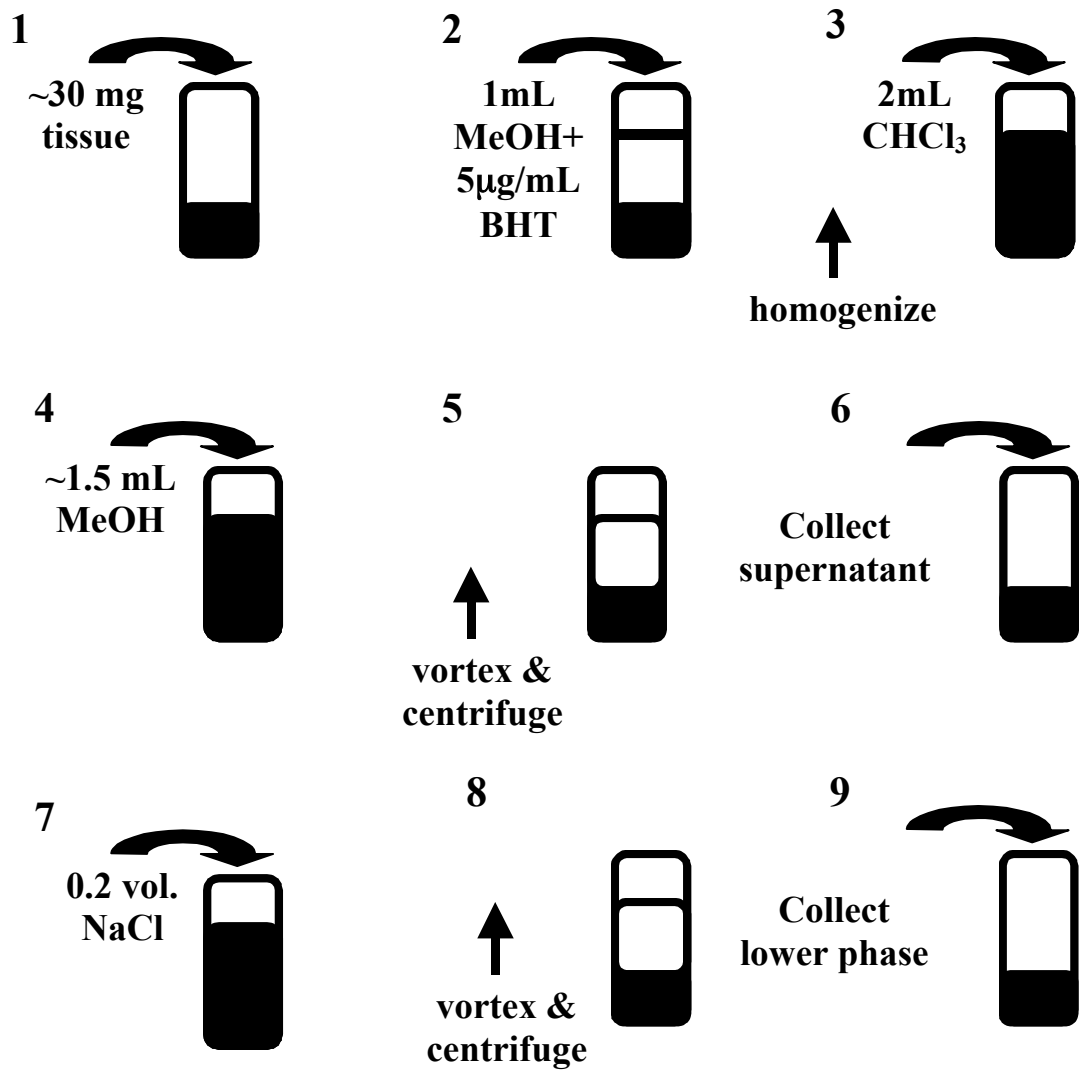

Fig. 8. ***SkM lipid extraction procedures.*** **(1) For analysis of lipid species, tissues were crushed while under liquid nitrogen and (2) homogenized in ice-cold (80%) methanol (MeOH)/H_2O containing butylated-hydroxytoluene (BHT, 5μg/mL). (3) The MeOH/H_2O homogenate was mixed with chloroform ($CHCl_3$) (2:1 v/v $CHCl_3$:MeOH). (4) The sample was homogenized 2 x 10 *s* and ~1.5 mL MeOH was added to bring the sample to a single phase. (5) Samples were centrifuged at 3,000 rpm for 30 minutes to spin down protein pellet. (6) The supernatant was removed without disturbing the protein pellet and (7) 0.2 volumes of 0.1 N sodium chloride added. (8) The solution was vortexed for 30 seconds and centrifuged at 1500 rpm for 10 minutes. (9) The bottom lipid-containing layer was removed, evaporated using a speed vacuum and stored at -80°C.**

2. Measurement of protein content

The pellet remaining from the lipid extraction procedure was allowed to air-dry for 20-30 minutes. A volume of 1 mL 1 N sodium hydroxide (NaOH) was added and samples incubated in a 60°C water-bath for 1h to dissolve the pellet. Protein content was determined using a colormetric assay kit (Pierce, Rockford, IL). Briefly, samples were diluted 5X with 0.1 N NaOH and a volume of 10 μL of the diluted sample was added to a 96-well micro-plate in triplicate. To the samples and standards (range 0-2 mg/mL) a 200 μL volume of working solution (8:1 reagent A:reagent B) was added and the plate was incubated at 37°C for 30 minutes. Absorbance was measured using an Emax Micro-plate Reader (Molecular Devices Corporation, Sunnyvale, CA) and quantified using Softmax Pro (Molecular Devices Corporation, Sunnyvale, CA) software. The mean of the triplicate absorbance was used to manually calculate protein concentrations from the standard curve equation.

3. Measurement of skeletal muscle diacylglycerol and ceramide content

DAGs and ceramides were isolated and separated by thin layer chromatography (TLC) with silica gel plates as described previously (43). Briefly, dried lipid samples were resuspended in 500 μL of $CHCl_3$ and aliquots of the solution of neutral lipid (50 μL in duplicate) and standards (range, 0-2000 pMol/100 μL) were dried under a vacuum. A volume of 110 μL of radiolabeled reaction mix (50 μL reaction buffer (0.1 M imidazole, 0.1 M NaCl, 25 mM $MgCl_2$, 2 mM EGTA, pH=6.6), 20 mM dithiothreitol (DTT), 5 mM ATP, 20 μL detergent (7.5% n-octyl-β-glucopyranoside (w/v), 5 mM cardiolipin, 1 mM diethylenetriaminepentaacetic (DETAPAC)), 5 μg DAG Kinase (Cal Biochem, San Diago, CA), 5 μL enzyme diluent (0.01 M imidazole, 1 mM DETAPAC, pH=6.6), and 1.25 μCi γ-^{32}P-ATP) was added to each sample and standard. Following a series of incubations at 37°C

and sonications, 1% perchloric acid (PCA) was added to stop the DAG Kinase reaction. The samples were mixed with 2:1 MeOH/$CHCl_3$ and incubated at room temperature for 10 minutes. $CHCl_3$ and 1% PCA were then added, samples vortexed and centrifuged at 2000 x *g* for 1 minute to remove the unreacted ^{32}P-ATP. The supernatant was discarded and the sample washed twice (vortex for 3 x 5 seconds, centrifuge at 2000 x *g* for 1 minute, and remove supernatant) with 1 mL 1% PCA. The bottom layer containing ^{32}P-DAG and ceramide was collected and dried under a vacuum. To the dried sample, 25 μL of 95:5 (v/v) $CHCl_3$:MeOH was added, the samples spotted onto TLC plates and placed into a TLC migration tank for ~3h. The mobile phase consisted of $CHCl_3$:MeOH:acetic acid (65:15:5 v/v/v). TLC plates were exposed to film overnight at -80°C to allow determination of migration of ^{32}P labeled lipid species (DAG and ceramide). ^{32}P-DAG and ceramide were scraped into a 20 mL scintillation vial, 10 mL of scintillation cocktail was added and vials were counted for 1 minute. Lipid species concentrations were calculated as nMol per μg protein, determined from the migration of known concentrations for DAG and ceramide. Procedures are summarized in Fig. 9.

4. Measurement of skeletal muscle triglyceride content

SkM TG concentrations were determined using a colorimetric assay as previously described (7) with modifications. Briefly, a 200 μL aliquot of extracted lipids was placed into a glass sample tube and allowed to air-dry overnight. To the dried sample, 40 μL of Triton X-114:MeOH (2:1 v/v) and 60 μL of tert-butanol were added and vortexed. A 5 μL aliquot of sample (in duplicate) and known standards were added to 1.5 mL acrylic cuvettes (PGC Scientific, Frederick, MD). To the samples and standards, 500 μL of prewarmed (37°C) INFINITY triglyceride reagent (Sigma, St. Louis, MO) was added, mixed thoroughly,

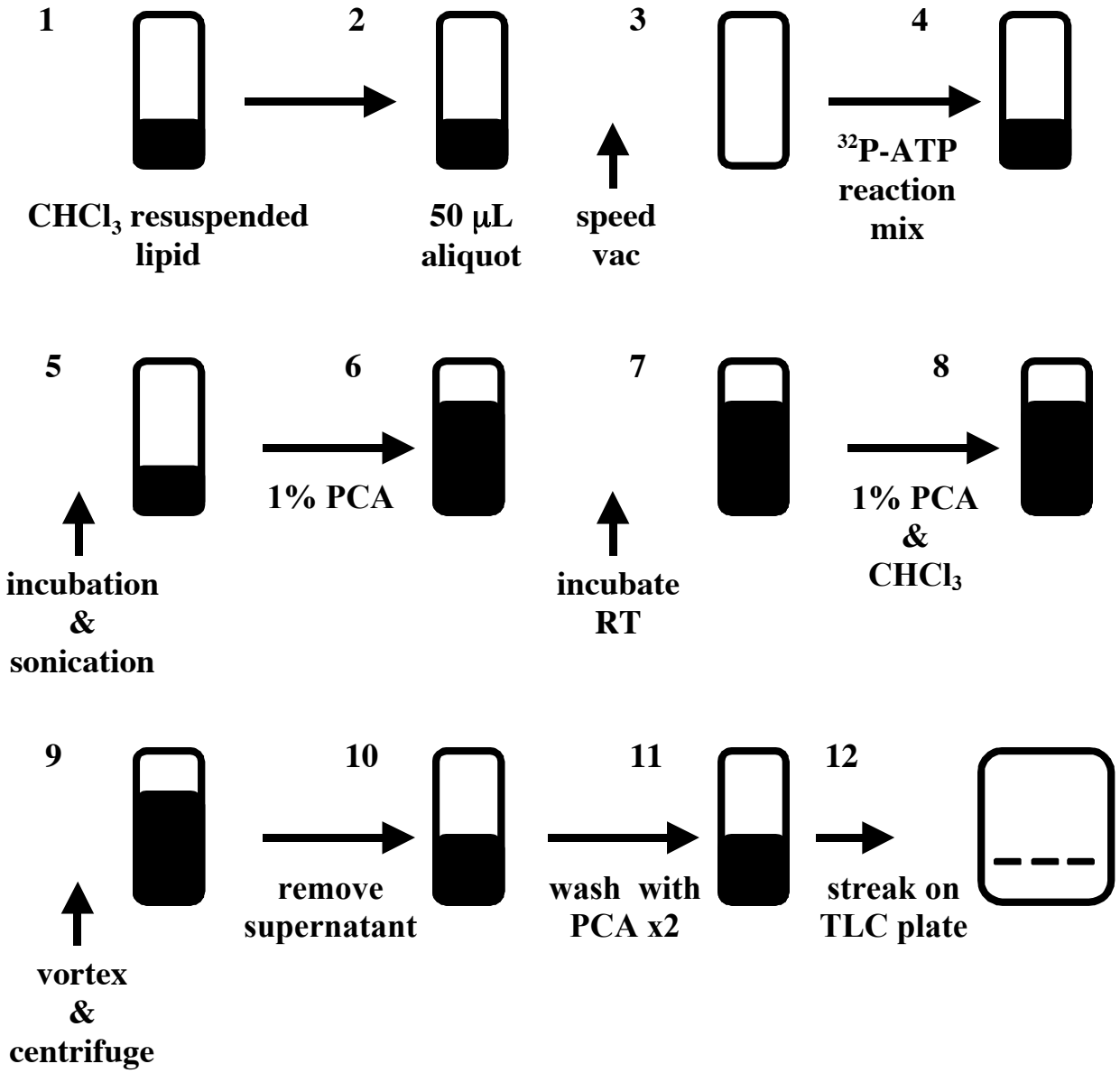

Fig. 9. ***DAG and ceramide isolation method.*** **(1) Dried lipid samples were resuspended in 500 µL of $CHCl_3$ and (2) aliquots of the solution of neutral lipid and standards were (3) dried under a vacuum. (4) A volume of 110 µL of radiolabeled reaction mix was added to each sample and standard. (5) Following a series of incubations at 37°C and sonications, (6) 1% perchloric acid (PCA) was added to stop the DAG Kinase reaction. (7) The samples were mixed with 2:1 MeOH/$CHCl_3$ and incubated at room temperature for 10 minutes. (8) $CHCl_3$ and 1% PCA were then added, (9) samples vortexed and centrifuged at 2000 x *g* for 1 minute (10) to remove the unreacted ^{32}P-ATP. (11) The supernatant was discarded and the sample washed twice with 1 mL 1% PCA. The bottom layer containing ^{32}P-DAG and ceramide was collected and dried under a vacuum. (12) To the dried sample, 25 µL of 95:5 (v/v) $CHCl_3$:MeOH was added, the samples spotted onto TLC plates and placed into a TLC migration tank for ~3h. Lipid species concentrations were calculated as nMol per µg protein, determined from the migration of known concentrations for DAG and ceramide.**

and incubated at 37°C for 5 minutes. Absorbance at 520 nm was measured for samples and standards using a Beckman DU530 spectrophotometer (Beckman, Fullerton, CA). TG content was calculated as μg/mg protein.

5. Adenovirus purification

Leptin adenovirus was purified as described by Chen *et al.* (9). A 1 mL liquid nitrogen cytostock of human embryonic kidney (293 HEK) cells was plated onto a 10-cm cell culture plate containing 9 mL media (Dulbecco's modification of eagle's medium, Mediatech, VA) with additions (50 mL fetal bovine serum (Invetrogen, Grand Island, NY) and 10 mL penicillin/stretomyocin (Invetrogen, Grand Island, NY) per 500 mL media) and incubated at 37°C. Cell were allowed to proliferate until they reached ~100% confluence and then divided equally into 4 10-cm plates. This process was followed again yielding 16 10-cm plates of 293 cells. When the cells achieved ~100% confluence, the cells were transferred 1:1 to 25-cm plates. Finally, at ~80% confluence, cells were infected with crude (unpurified) virus. Procedures for cell culture are summarized in Fig. 10.

Approximately 48-72h later, lysed cells were collected and the virus purified. Purification procedures are summarized in Fig. 11. Briefly, 0.5% volume of non-ionic detergent was added to the cell lysate, shaken gently at room temperature for 10 minutes, and centrifuged for 15 minutes at 20,000 x *g* to pellet out cell debris. To the collected supernatant, a 0.5 volume of solution of 20% polyethylene glycol/2.5 M NaCl was added and samples were shaken on ice overnight. The samples were centrifuged for 15 minutes at 20,000 x *g* and the supernatant discarded. The precipitated virus on the wall of the bottle was resuspended in 2.5-4.0 mL PBS, transferred into 3 mL ultracentrifuge tubes (Hitachi, Japan), and centrifuged for 10 minutes at 20,000 x *g* to remove cell debris. To the recovered

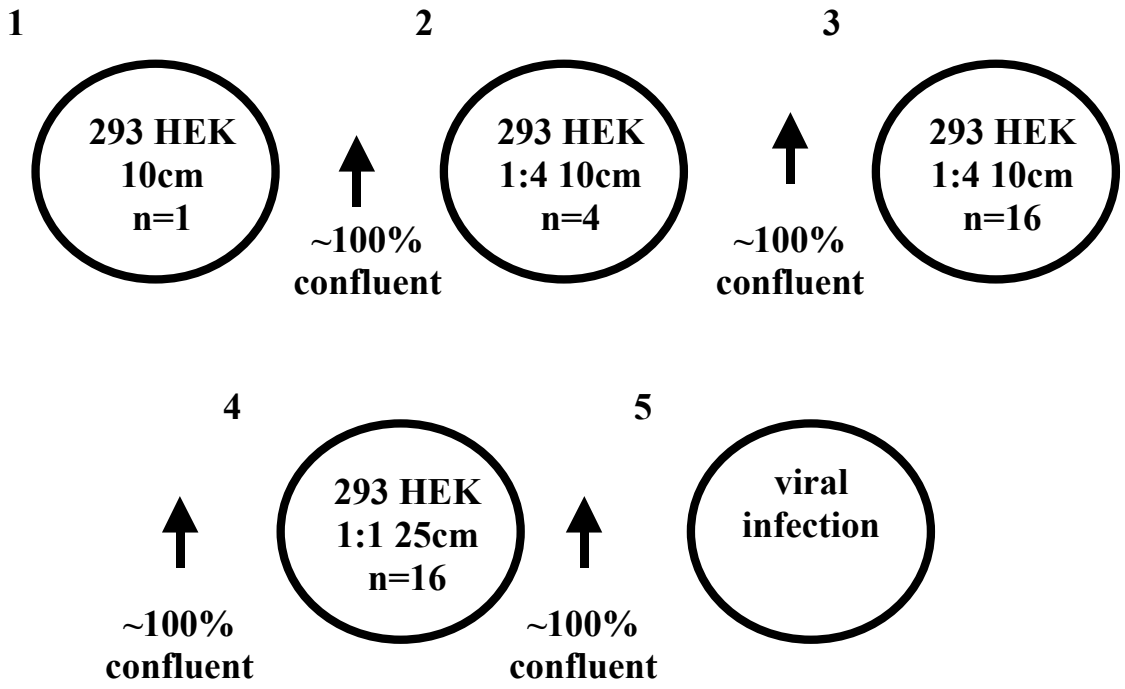

Fig. 10. ***Cell culture for adenovirus preparation.*** **(1) A 1 mL liquid nitrogen cytostock of human embryonic kidney (293 HEK) cells was plated onto a 10-cm cell culture plate containing 9 mL media (DMEM) with additions and incubated at 37°C. (2) Cell were allowed to proliferate until they reached ~100% confluence and then divided equally into 4 10-cm plates. (3) This process was followed again yielding 16 10-cm plates of 293 cells. (4) When the cells achieved ~100% confluence, the cells were transferred 1:1 to 25-cm plates. (5) Finally, at ~80% confluence, cells were infected with crude virus.**

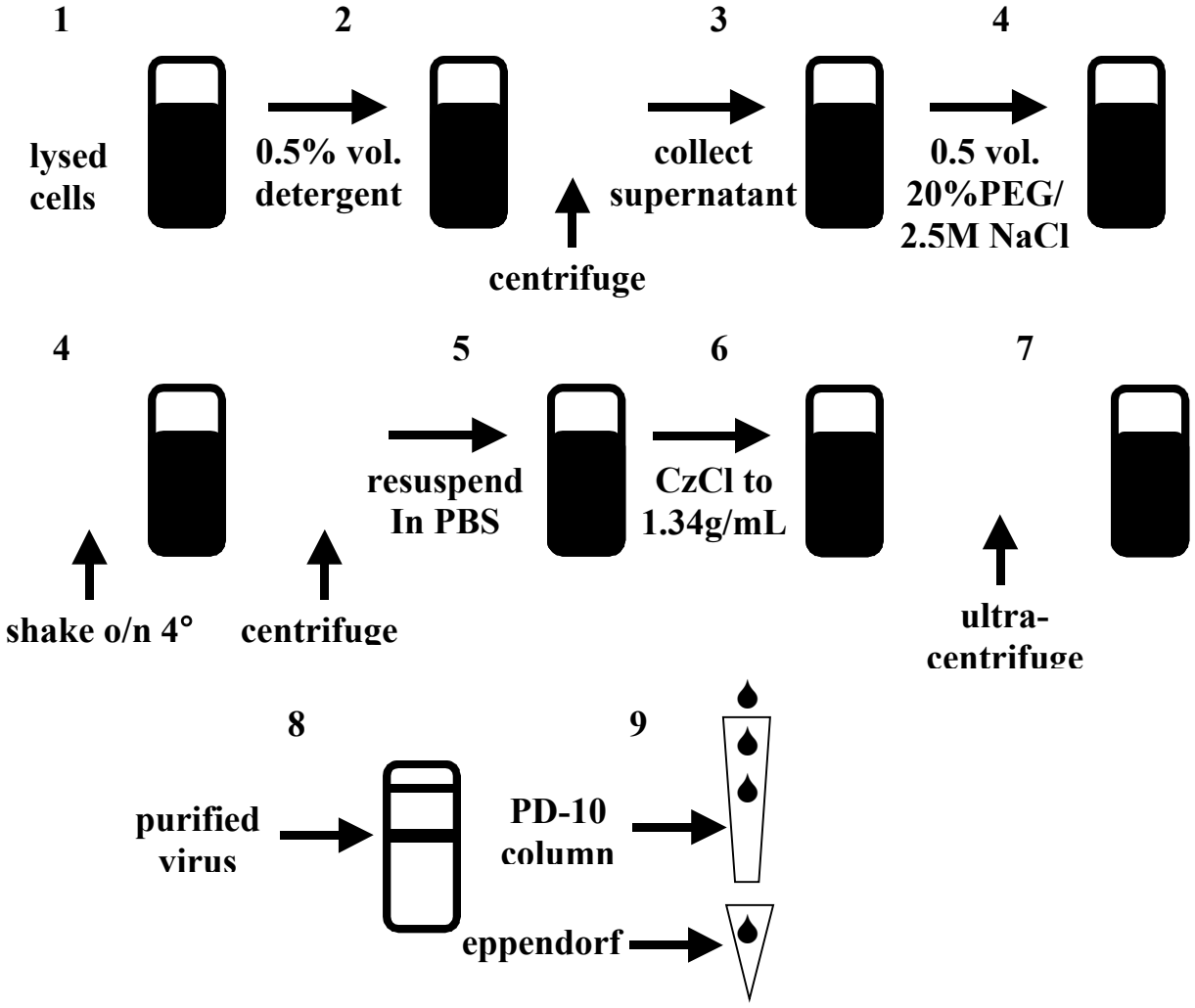

Fig. 11. ***Adenovirus purification procedures.*** **(1) Approximately 48-72h after infection with crude virus, lysed cells were collected and the virus purified. (2) A 0.5% volume of non-ionic detergent was added to the cell lysate, shaken gently at room temperature for 10 minutes, and centrifuged for 15 minutes at 20,000 x *g* to pellet out cell debris. (3) To the collected supernatant, (4) a 0.5 volume of solution of 20% polyethylene glycol (PEG)/2.5 M NaCl was added and (4) samples were shaken on ice overnight. The samples were centrifuged for 15 minutes at 20,000 x *g* and the supernatant discarded. (5) The precipitated virus was resuspended in 2.5-4.0 mL PBS, transferred into 3 mL ultracentrifuge tubes, and centrifuged for 10 minutes at 20,000 x *g*. (6) To the recovered supernatant, cesium chloride (CzCl) was added to achieve a final density of 1.34 g/mL. (7) The samples were ultracentrifuged at 90,000 rpm for 3h at 25°C. (8) Infectious virus was collected (~1 mL) and (9) fractionated through a PD-10 desalting column. Ten-drop fractions were collected in 1.5 mL eppendorf tubes containing 70 µL of sterile 70% glycerol. To determine virus yield, 2 µL of the drop fraction was added to 98 µL of PBS and read by spectrophotometer (OD 260 nm). The highest OD fractions were pooled and absorbance measured again. Virus titer (particles/mL) was calculated by multiplying the OD by 50. Aliquots were stored at -80°C.**

supernatant, cesium chloride (~0.55g/mL) was added to achieve a final density of 1.34 g/mL. The samples were ultracentrifuged (Sorvall RC M120 GX, Kendro Lab Products, Newtown, CT) at 90,000 rpm for 3h at 25°C. Infectious virus was collected (~1 mL) and fractionated through a PD-10 desalting column (Amersham Biosciences, Piscataway, NJ). Ten-drop fractions were collected in 1.5 mL eppendorf tubes containing 70 μL of sterile 70% glycerol. To determine virus yield, 2 μL of the drop fraction was added to 98 μL of PBS and read by spectrophotometer (OD 260 nm). The highest OD fractions were pooled and absorbance measured again. Virus titer (particles/mL) was calculated by multiplying the OD by 50. Aliquots were stored at -80°C.

6. Measurement of plasma leptin

Circulating leptin levels were analyzed from plasma samples using a rat leptin radioimmunoassay kit (Linco Research Immunoassay, St. Charles, MO). This assay consisted of a 3-day protocol as follows. Day 1, to a mix of assay buffer and rat leptin antibody, a volume 25 μL of plasma (in duplicate) was added, vortexed and incubated overnight at room temperature. Day 2, radiolabeled rat leptin (^{125}I) was added, the sampled vortexed, and incubated overnight at room temperature. Day 3, cold precipitating reagent was added, samples vortexed, and incubated for 20 minutes at 4°C. The samples were then centrifuged 3,000 x *g* for 1h at 4°C. The supernatant was decanted, allowed to air-dry for approximately 1h, and the product counted in a gamma counter. Circulating leptin levels were calculated as ng/mL.

7. Measurement of fatty acid oxidation in isolated soleus muscle

Following an overnight fast, rats were anesthetized under isoflurane and SOL muscles were quickly excised. Muscles were placed in a pregased (95% O_2, 5% CO_2) 37°C 6-well

plate containing 3 mL KRH-buffer for 20-minutes and gently shaken. Following the equilibration period, the muscles were moved to a well containing 3 mL KRH-buffer and ^{3}H-palmitate (0.5μCi/mL) for 60-minutes. As the ^{3}H-palmitate is taken up and oxidized by the isolated muscle, one of the by products is $^{3}H_2O$ in the incubation media. A 200μl aliquot of incubation media was taken and placed into an uncapped 1.5 mL eppendorf tube. The tube was placed into a 20 mL scintillation vial containing 500 μL distilled/deionized water. The vial was capped and placed into a 50°C oven and incubated overnight allowing for the equilibration of $^{3}H_2O$ (by evaporation and condensation) into the scintillation vial. Following the overnight equilibration, the eppendorf tube was removed, 10mL of scintillation fluid was added to the vial, and counted for $^{3}H_2O$ activity. Oxidation was calculated as μMol palmitate/g tissue/h.

8. Measurement of fatty acid transporters and plasma membrane fatty acid binding protein

Approximately 300 mg of GAS tissue was shipped in dry ice to Dr. Bonen for analysis of FAT/CD36 and FABPpm. Whole muscle homogenates (50 μg protein) from GAS were separated on 12% SDS-polyacrylamide gels (150 V for 1h). Proteins were transferred to immobilon polyvinylidene difluoride membranes (100 V, 90min) and incubated overnight with 10% blocking buffer. Membranes were then incubated for 2h with either FAT/CD36 or FABPpm antibody. Following a series of washes, membranes were incubated for 1h with donkey anti-rabbit immunoglobulin G horseradish peroxidase-conjugated secondary antibody. FAT/CD36 and FABPpm were detected by an enhanced chemiluminescence detection method.

9. Measurement of phosphorylated acetyl-CoA carboxylase

Fatty acid oxidation is allosterically regulated by acetyl-CoA carboxylase (P-ACC) and intracellular formation of Malonyl-CoA, a potent regulator of FAox. Changes in P-ACC were measured from βGal and HLEP treated rats following both 3h and 6h Intralipid infusion. Male Wistar rats were catheterized in the carotid artery and randomly assigned to one of four treatment protocols: (1) βGal 3h LIP, (2) HLEP 3h LIP, (3) βGal 6h LIP, or (4) HLEP 3h LIP. Following the infusion period, rats were anesthetized, tissues extracted, and quickly frozen for analysis. P-ACC protein was measured in SkM extracts by western blot analysis using anti-bodies specific for P-ACC (Cell Signaling Technology, Beverly, MA). Fine powder crushed tissues were homogenized in ice-cold cell lysis buffer containing protease inhibitors (1 mM sodium vanadate, 1 μg/mL leupeptin, 1 mM phenylmethylsulphonyl (PMSF), and 3 TIU/mL Aprotinin). Following centrifugation, the supernatant was collected and protein concentrations determined as previously described. A volume of 100 μg protein/40 μL was loaded on a 5% SDS-PAGE gel. Samples were run at 180V for 75 minutes and then transferred to nitrocellulose membranes at 260 mA for 2.5h. Membranes were blocked for 2h with 5% blocking buffer (2.5 g non-fat dry milk in 50 mL TBST). Primary antibody was diluted 1:800 in 10 mL of 1% blocking buffer, added to the membrane, and incubated overnight at 4°C. Following a series of washes with TBST, the secondary antibody (anti-rabbit, Cell Signaling Technology, Beverly, MA) was diluted 1:5000, added to the membrane and incubated at room temperature for 1h. The membrane was washed again (3 x 10 minutes) with TBST and proteins were visualized with chemiluminescence reagents according to the manufacture's protocol (Cell Signaling Technology, Beverly, MA). Band intensities were quantified using densitometry software

(Image J, National Institute of Mental Health, Bethesda, Maryland). To determine differences, all band intensities were standardized to the βGal group. As a loading control, a volume of 100 μg protein/40 μL was loaded on a 10% SDS-PAGE gel. Samples were run and transferred as previously described. Following the 2h incubation in 5% blocking buffer, the primary antibody tubulin (Cal Biochem, San Diego, CA), a housekeeping protein, was diluted 1:1000 in 1% blocking buffer, added to the membrane and incubated overnight at 4°C. The secondary antibody (anti-mouse, Cell Signaling Technology, Beverly, MA) was diluted 1:5000, added to the membrane and incubated at room temperature for 1h. The membrane was washed and proteins were visualized with chemiluminescence reagents according to the manufacture's protocol (Cell Signaling Technology, Beverly, MA).

10. Measure of gene expression

In addition to changes in protein concentration of P-ACC, FAT/CD36 and FABPpm, it was of interest to examine SkM gene expression changes associated with leptin treatment. Gene transcripts of interest included Sterol Regulatory Element Binding Protein-1c (SREBP-1c), which regulates fatty acid synthesis, Uncoupling Protein-3 (UCP-3), due to its role in thermogenesis, and Acetyl CoA Carboxylase-2 (ACC2) as an allosteric regulator of Malonyl CoA and fatty acid oxidation. Gene expression was assessed by reverse transcriptase-polymerase chain reaction (RT-PCR). Briefly, ~100 mg of crushed SOL tissue was homogenized in 1 mL of Trizol (Invetrogen, Grand Island, NY). Samples were incubated at room temperature for 15 minutes. A 0.2 volume of $CHCl_3$ was added, samples shaken vigorously by hand for 15 seconds, and incubated for 5 minutes at room temperature. The homogenate was centrifuged at 12,000 x *g* at 4°C for 15 minutes. The upper aqueous phase containing RNA was collected and 0.5 mL of isopropyl alcohol per 1 mL Trizol was added to

precipitate out the RNA. Samples were incubated for 10 minutes at room temperature and centrifuged at 12,000 x *g* at 4°C for 15 minutes. The supernatant was discarded and 75% ethanol added to wash the pellet. Following a centrifugation at 7,500 x *g* at 4°C for 5 minutes, the supernatant was discarded and the remaining RNA pellet allowed to air-dry (~30 minutes). Finally, the pellet was dissolved in 20 μL DepC treated water. RNA concentration was determined by spectrophotometer (OD 260 nm).

cDNA was synthesized from isolated RNA using a commercially available kit (Advantage RT-for-PCR Kit, BD Biosciences, Palo Alto, CA). Isolated RNA (1 μg) and DepC treated water (total volume 12.5 μL) were mixed and 1 μL oligo DT primers added. The RNA was heated at 70°C for 2 minutes and then quickly quenched on ice. To the sample, 6.5 μL of reaction mix (4.0 μL 5x Reaction Buffer, 1.0 μL 10 mM dNTP mix, 0.5 μL Recombinant RNase Inhibitor, and 1.0 μL MMLV reverse transcriptase) was added and mixed thoroughly. The samples were incubated at 42°C for 1h and the heated at 94°C for 2 minutes to stop the cDNA synthesis. A volume of 80 μL of DepC water was added to the samples and stored at -80°C. The synthesized cDNA was used for all RT-PCR reactions. PCR conditions were optimized for each gene transcript and linearity experiments run to determine optimal cycle length. Following thermocycling with forward and reverse primers specific for the genes of interest, 10 μL of 10 x sample buffer was added, samples briefly centrifuged, and a volume of 15 μL loaded on to a 1.5% agarose gel containing ethidium bromide. Electrophoresis was completed for 1h at 150V. Bands were viewed under UV light and a Polaroid picture taken analysis. Band intensities were analyzed using densitometry software (Image J, National Institute of Mental Health, Bethesda, Maryland) and standardized to the housekeeping gene β-Actin.

11. Fractionation and measurement of PKCθ

Briefly, muscles (100 mg tissue) were homogenized in 400μl of ice-cold Buffer A (20 mmol/l MOPS, pH=7.5, 250 mMol/L mannitol, 1.2 mMol/L EGTA, 1 mMol/L dithiotheitol (DTT), 2 mMol/L PMSF, 200 mg/mL leupeptin, and 2 mMol/L benzamidine). The homogenate was centrifuged at 100,000 x *g* for 45 minutes at 4°C and the supernatant (cytosolic fraction) was removed and kept for protein determination. The pellet was washed once with Buffer A and recentrifuged at 100,000 x *g* for 45 minutes at 4°C. The supernatant was discarded and the protein pellet was resuspended in 400 μL of Buffer B (20 mMol/L MOPS, pH=7.5, 0.5% (wt/vol) decanoyl-N-methyl-glucamide, 2 mMol/L EDTA, 5 mMol/L EGTA, 1 mMol/L DTT, 2 mMol/L PMSF, 200 mg/mL leupeptin, and 2 mMol/L benzamidine). Following 1h of gentle rocking at 4°C, the extract was centrifuged at 100,000 x *g* for 45 minutes at 4°C. The resulting supernatant contained the membrane fraction. Procedures are summarized in Fig. 12.

Protein content was determined for both cytosolic and membrane fractions as previously described. The samples (50μg protein) were electrophoresed on 10% SDS-PAGE and run for 60 minutes at 180 V. Proteins were then transferred to nitrocellulose membranes for 2.5h at 260 mA. Following a 2h incubation with 5% blocking buffer, the membranes were immunoblotted overnight using anti-PKCθ antibody (Santa Cruz Biotechnology, Santa Cruz, CA). The proteins were visualized with chemiluminescence reagents according to the manufacture's protocol. Band intensities were quantified using densitometry software (Image J, National Institute of Mental Health, Bethesda, Maryland). To determine differences, all band intensities were standardized to the βGal group. Finally, total PKCθ was calculated by adding the standardized OD from the membrane and cytosolic fractions.

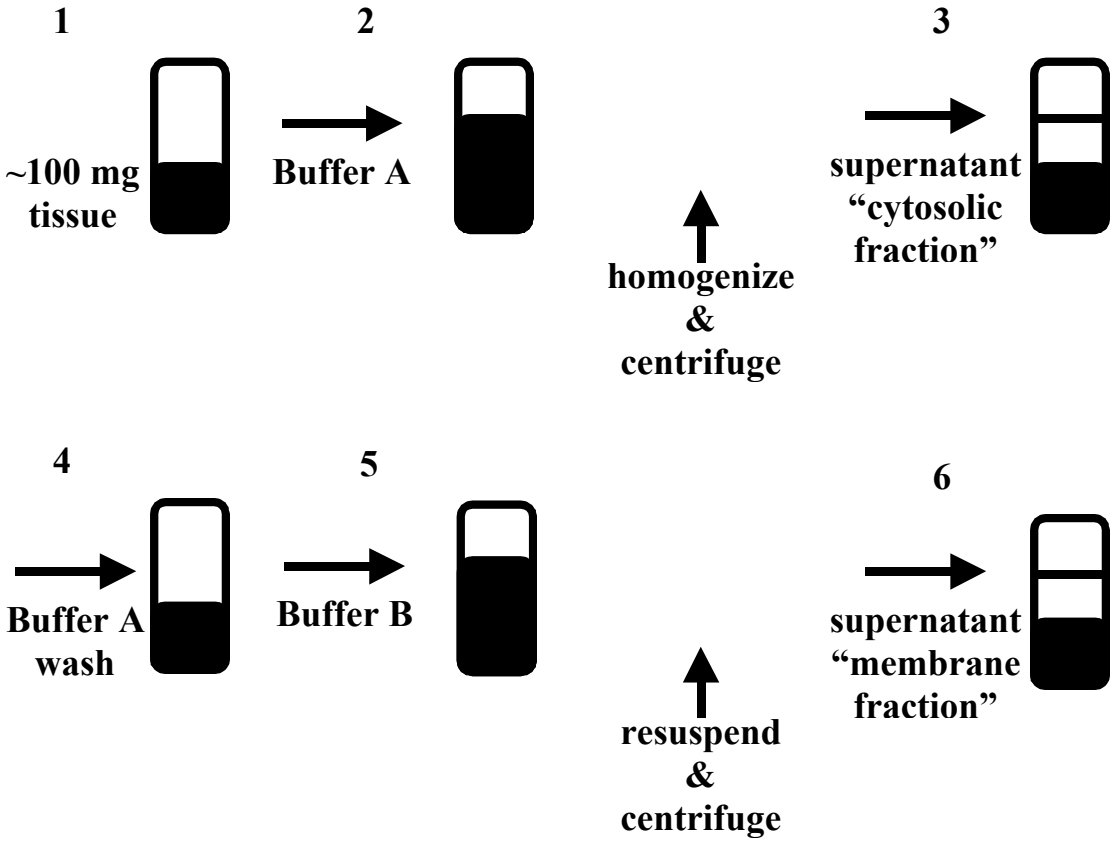

Fig. 12. ***PKCθ fractionation procedures.*** **(1) Muscles (100 mg tissue) were homogenized in (2) 400µl of ice-cold Buffer A. (3) The homogenate was centrifuged at 100,000 x *g* for 45 minutes at 4°C and the supernatant (cytosolic fraction) was removed and kept for protein determination. (4) The pellet was washed once with Buffer A and recentrifuged at 100,000 x *g* for 45 minutes at 4°C. (5) The supernatant was discarded and the protein pellet was resuspended in 400 µL of Buffer B. Following 1h of gentle rocking at 4°C, the extract was centrifuged at 100,000 x *g* for 45 minutes at 4°C. (6) The resulting supernatant contained the membrane fraction.**

12. Measurement of 2-deoxyglucose uptake in denervated skeketal muscle

Forty-eight hours following denervation, food was withdrawn for 24-h. Rats were then weighed and anesthetized under isoflurane. The SOL muscle from the denervated hindlimb and the contralateral side were excised and subjected to insulin-stimulated 2-deoxyglucose (2-DG) uptake incubation (7). Briefly, muscle were incubated in a series of Krebs-Ringer-Henseleit (KRH) buffer (11.8 mM NaCl, 1.19 mM KH_2PO_4, 4.76 mM KCl, 1.19 mM $MgSO_4$, 24.9 mM $NaHCO_3$, 1.2 mM $CaCl_2$, 0.1% fat-free BSA) with additions, in a pre-gassed (95% O_2, 5% CO_2) 29° C shaking water-bath. The muscles were first incubated in 3 mL KRH buffer containing 8 mM glucose and 1 mM mannitol for 30-min and then 1 mM mannitol for 10-min. Muscles were then transferred to KRH containing 1 mM ^{14}C-mannitol (0.32 μCi/ml) and 1 mM ^{3}H-2-deoxyglucose (1 μCi/mL) in the presence of insulin at a final concentration of 100 mU/ml. The muscles were then digested in 3 mL of 1 N NaOH in 70°C oven of 1-h. A 200-μL aliquot was assayed for radioactivity in scintillation fluid and 2-DG uptake was calculated as nanomoles of 2-DG per μL of intracellular (IC) water space.

IV. Statistical analysis

All data are expressed as mean ± SEM. Group comparisons were made using Student's t-test. Significance was set *a priori* at $P<0.05$.

V. Results

A. Intralipid induces insulin resistance

Using an animal model, specific aim 1 set to confirm that exogenous lipid infusion elicits IR and evaluate associated changes in SkM lipid species in various fiber types. Previous reports have demonstrated resultant IR elicited by acute hyperlipidemia (lipid infusion) (4, 15, 27, 31, 44). Because the primary aim of this investigation was the examination of

mechanisms associated with improvements on insulin action by leptin, it was first necessary to establish that indeed lipid infusion elicits IR in our animal model. Additionally, it was of particular interest to examine SkM lipid species content, specifically DAG, ceramide, and TG, in various fiber types. To address specific aim 1, six groups of animals were used. Hyperinsulinemic-euglycemic clamps were used to determine whole body insulin sensitivity in male Wistar rats following a 5h Intralipid (LIP, 5 mL/kg/h, n=6) infusion (Fig. 2). Control rats were infused with saline (SAL, 5 mL/kg/h, n=6) prior to the clamp. An increase in SkM lipid content (i.e. DAG, ceramide, and TG) was examined in male Wistar rats following a 3h LIP (n=6) or 6h LIP (n=6) infusion. Controls for both SkM lipid content experiments received only SAL (Fig. 3).

Table 1 indicates basal variables from the 5h saline (SAL) and lipid (LIP) infused animals. Body weight (252±9.1 vs 262±20.4 g; P=0.54) and plasma glucose concentrations were not different between groups (all P>0.05). Rates of glucose infusion were significantly lower in LIP compared to SAL (31.9± 1.1 vs 38.5± 0.8 mg/kg/min; P=0.004) demonstrating the expected induction of whole body IR in response to a 5h infusion of Intralipid (Fig. 13).

Table 1. ***Basal variables from saline and lipid infused animals.***

	SAL n=6	LIP n=6
Weight, g	252±9.1	262±20.4
Plasma glucose, mg/dl		
Pre-infusion	127.8±2.4	109.8±1.8
Post-infusion	117.2±8.1	94.8±6.0
Post-clamp	116.4±2.6	124.0±3.4

Male Wistar rats were catheterized in the carotid artery and jugular vein, infused for 5-hours with either saline (SAL) or Intralipid/heparin (LIP), and insulin sensitivity determined using a 90-minute hyperinsulinemic-euglycemic clamp as described in Methods. Plasma glucose concentrations were measured prior to the 5h LIP or SAL infusion (Pre-infusion), immediately after the infusion (Post-infusion), and immediately following the clamp (Post-clamp). Data are mean ± SEM.

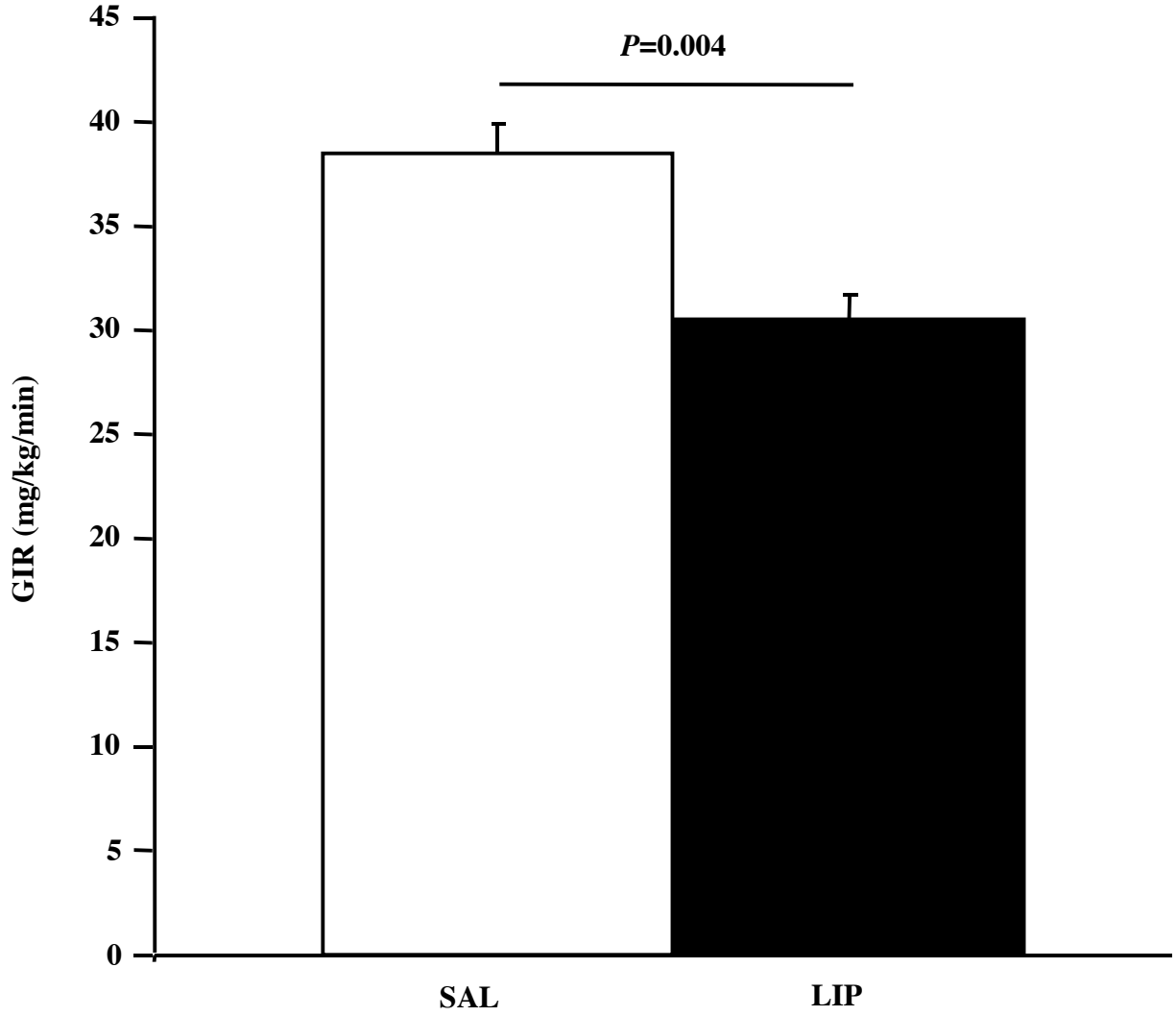

Fig. 13. ***Intralipid induced insulin resistance.*** **Male Wistar rats were catheterized in the carotid artery and jugular vein as described in Methods. Following recovery to presurgical body weight, rats were infused for 5h with either saline (SAL, 5 mL/kg/h, n=6) or Intralipid (LIP, 5 mL/kg/h, n=6). Insulin sensitivity was determined from a 90-minute hyperinsulinemic (15 mU/kg/min)-euglycemic clamp. Glucose infusion rate (GIR) was averaged from the last 60-min of the clamp. Data are mean ± SEM.**

B. Skeletal muscle lipid content is increased in response to Intralipid

Lipid content (DAG, ceramide, and TG) was measured in SOL, predominately type I fibers, from rats infused for 3h with SAL or LIP. DAG (2.8±0.2 vs 2.1±0.3 nMol/μg protein; *P*=0.04) and ceramide (0.8±0.1 vs 0.5±0.0 nMol/μg protein, *P*=0.02) in SOL from LIP were increased significantly compared to SAL (Fig. 14A, 14B). In contrast, TG content was significantly decreased in SOL (27.5±3.4 vs 41.0±5.7μg/mg protein; *P*=0.03) in LIP compared to SAL (Fig. 14C). Finally, lipid content of SOL from 6h infusions indicated no differences in DAG (2.6±0.2 vs 2.6±0.2 nMol/μg protein; P=0.91) or TG (19.5±2.2 vs 19.4±6.0 μg/mg protein; *P*=0.44) in LIP compared to SAL (Fig. 14A, 14C). However, significant differences were observed in ceramide (0.8±0.0 vs 0.6±0.1 nMol/μg protein; *P*=0.03) in LIP compared to SAL (Fig. 14B).

Acute hyperlipidemia (3h) induces increases in DAG and ceramides in soleus (SOL). Lipid content was measured in VAS and GAS from animals infused for 3h with either saline (SAL) or lipid (LIP) as described in Methods. Significant increases in VAS DAG (1.4±0.2 vs 0.9±0.2 nMol/μg protein; *P*=0.04) and ceramide (1.1±0.2 vs 0.6±0.1 nMol/μg protein; *P*=0.02) in LIP compared to SAL were observed (Fig. 15A, 15B). No differences were observed in TG content (36.1±5.0 vs 26.4±4.4 μg/mg protein; *P*=0.18) in LIP compared to SAL (Fig. 15C). A similar pattern was observed from GAS DAG (1.4±0.2 vs 0.9±0.2 nMol/μg protein; *P*=0.02) and ceramide (1.1±0.2 vs 0.6±0.1 nMol/μg protein; *P*=0.03) in LIP compared to SAL (Fig. 16A, 16B). No differences were observed in TG content (10.4±0.2 vs 8.4±1.1 μg/mg protein; *P*=0.07) in LIP compared to SAL (Fig. 16C).

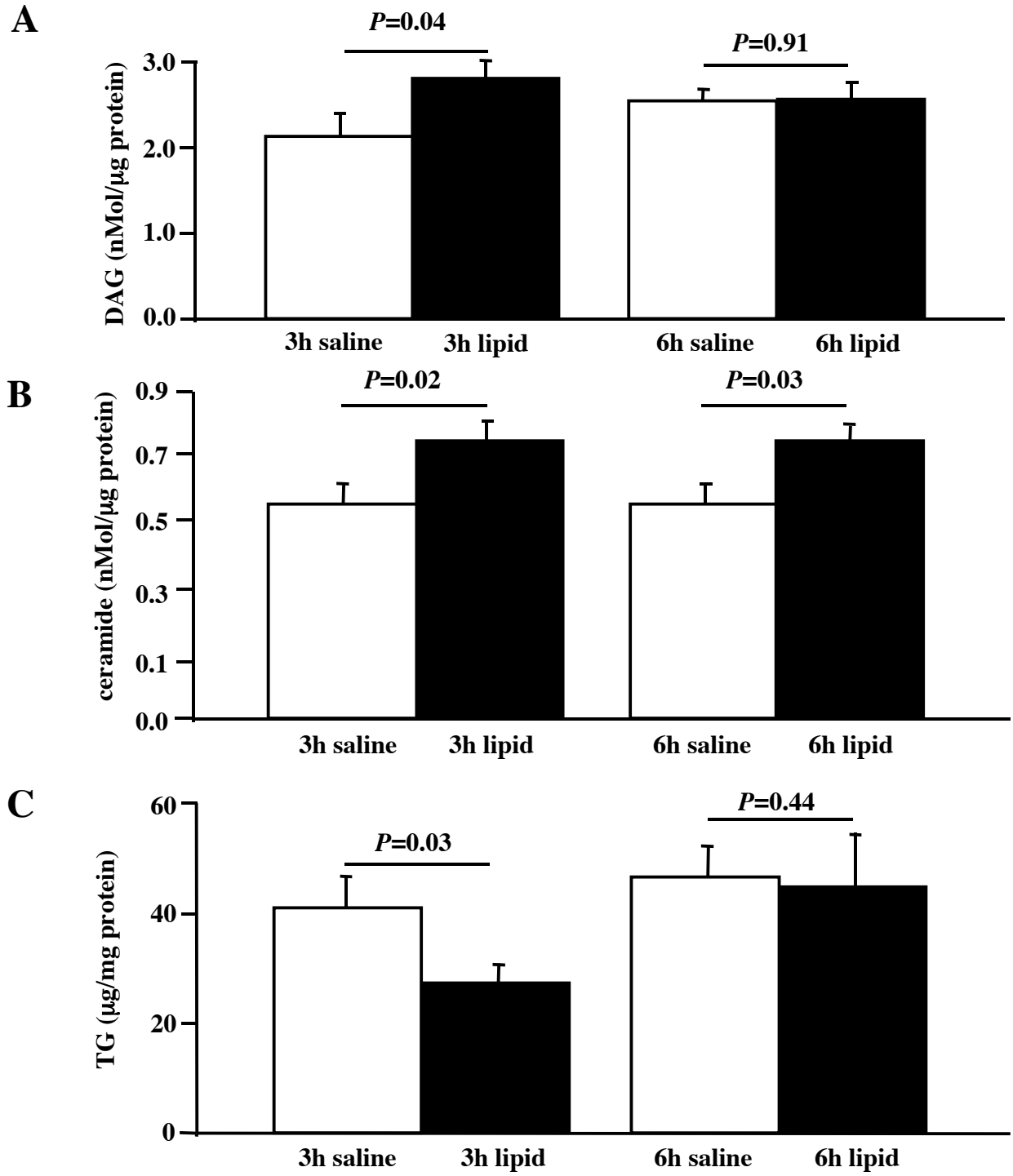

Fig. 14. ***Lipid content of soleus muscle following 3h and 6h Intralipid infusion.*** **Male Wistar rat were catheterized in the carotid artery as described in Methods. Following recovery to presurgical body weight, rats were infused for either 3h or 6h with either saline (5 mL/kg/h) or Intralipid (5 mL/kg/h)/heparin (6 U/h). Lipid species (*A*) DAG, (*B*) ceramide, and (*C*) TG content were measured in soleus muscle as described in Methods. Data are mean ± SEM; n=6/group.**

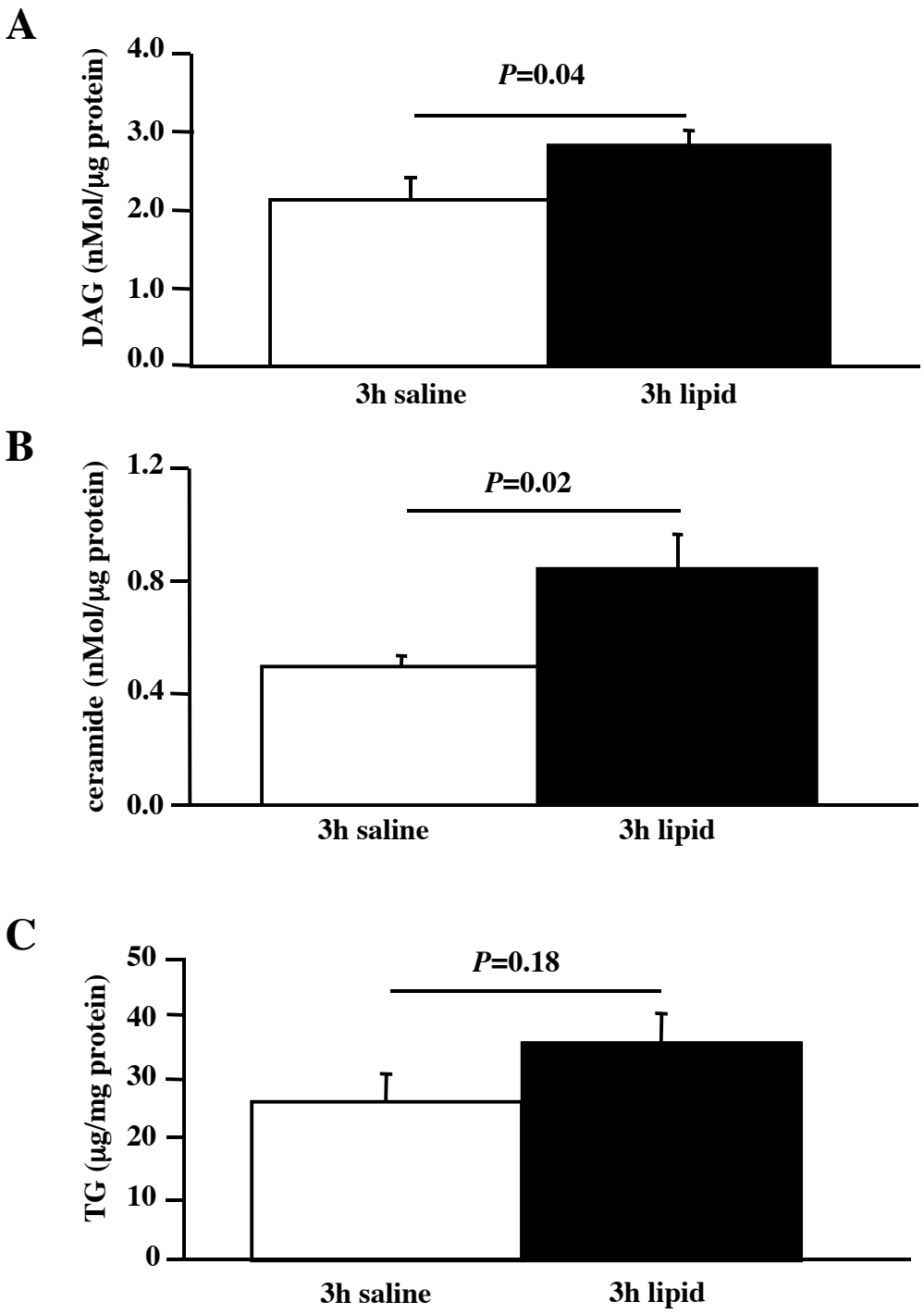

Fig. 15. ***Lipid content of superficial vastus muscle following 3h Intralipid infusion.*** **Male Wistar rat were catheterized in the carotid artery as described in Methods. Following recovery to presurgical body weight, rats were infused for 3h with either saline (5 mL/kg/h) or Intralipid (5 mL/kg/h)/heparin (6 U/h). Lipid species (*A*) DAG, (*B*) ceramide, and (*C*) TG content were measured in superficial vastus muscle as described in Methods. Data are mean ± SEM; n=6/group.**

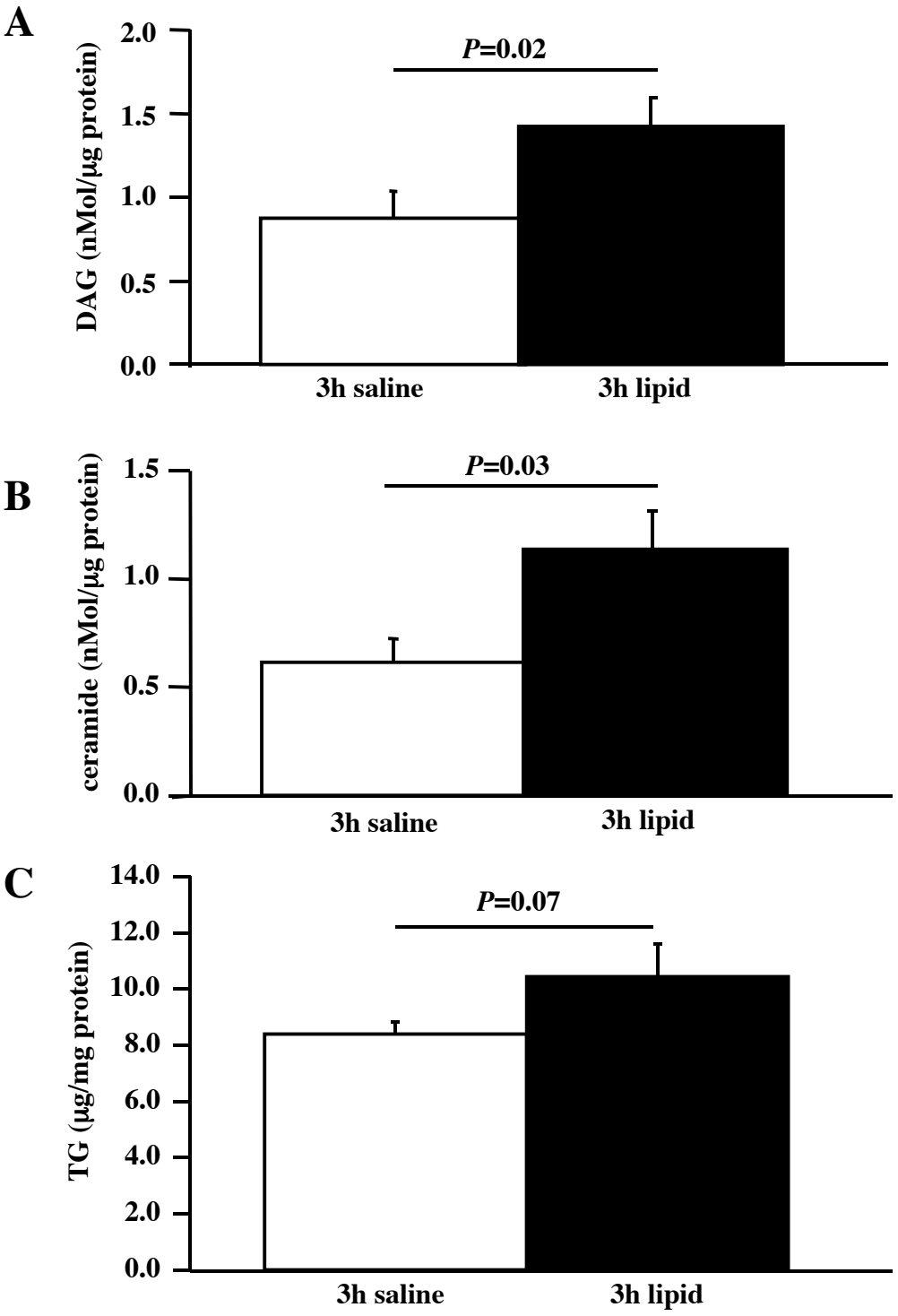

Fig. 16. ***Lipid content of gastrocnemius muscle following 3h Intralipid infusion.*** **Male Wistar rat were catheterized in the carotid artery as described in Methods. Following recovery to presurgical body weight, rats were infused for 3h with either saline (5 mL/kg/h) or Intralipid (5 mL/kg/h)/heparin (6 U/h). Lipid species (*A*) DAG, (*B*) ceramide, and (*C*) TG content were measured in gastrocnemius muscle as described in Methods. Data are mean ± SEM; n=6/group.**

C. Leptin prevents insulin resistance induced by Intralipid

Specific aim 2 was designed to address if chronic hyperleptinemia (HLEP) prevents the development of insulin resistance caused by lipid oversupply. Elevation of plasma FFA caused by the infusion of TG lipid emulsion induces IR by mechanisms not well understood (4, 15, 27, 31, 44). Defects seem to occur in SkM insulin stimulated glucose uptake, insulin signaling, and lipid content following a brief (3-5h) treatment period. Administration of leptin has been shown to improve insulin sensitivity in diet-induced and genetic models of IR (7, 11, 54). Likely mechanisms by which leptin improves IR include decreasing SkM lipid content, increasing FA oxidation, and increasing insulin-stimulated glucose uptake. However, it is unknown if leptin is able to prevent IR by acute hyperlipidemia.

Two groups of animals were used to address specific aim 2. Cannulas were chronically implanted into the carotid artery and jugular vein as described in Methods. Following recovery (3-5 days) to presurgical body weight, animals were administered via the carotid artery a recombinant adenovirus containing leptin. Food intake and body weight changes were monitored for 5d. Following an overnight fast, rats were infused for 5h with Intralipid and insulin sensitivity determined by a 90-minute hyperinsulinemic-euglycemic clamp (Fig. 3). As expected, no basal differences were observed between hyperleptinemic animals infused with saline (HLEP-SAL) or lipid (HLEP-LIP) for any variable (Table 2). Rates of glucose infusion were not different between HLEP-LIP and HLEP-SAL (Fig. 17; 43.0±1.9 vs 43.8±2.3 mg/kg/min; P=0.40) demonstrating that leptin is able to prevent IR induced by acute hyperlipidemia.

Table 2. ***Basal variables from saline and lipid infused hyperleptinemic animals***

	HLEP-SAL n=6	HLEP-LIP n=6
Weight, g	258±9.3	253±5.4
Plasma leptin (ng/mL)	53.0±5.9	62.7±4.7
Epididymal fat (g)	1.8±0.2	2.0±0.3
Mean food intake (g)	12.8±1.7	11.5±1.3

Male Wistar rats were catheterized in the carotid artery and jugular vein as described in Methods. Following recovery from surgery, rats were I.V. infused with adenovirus containing rat leptin cDNA (HLEP) and assigned to either 5h saline (HLEP-SAL) or Intralipid (HLEP-LIP) infusion. Insulin sensitivity was determined using a 90-minute hyperinsulinemic-euglycemic clamp as described in Methods. Data are mean ± SEM.

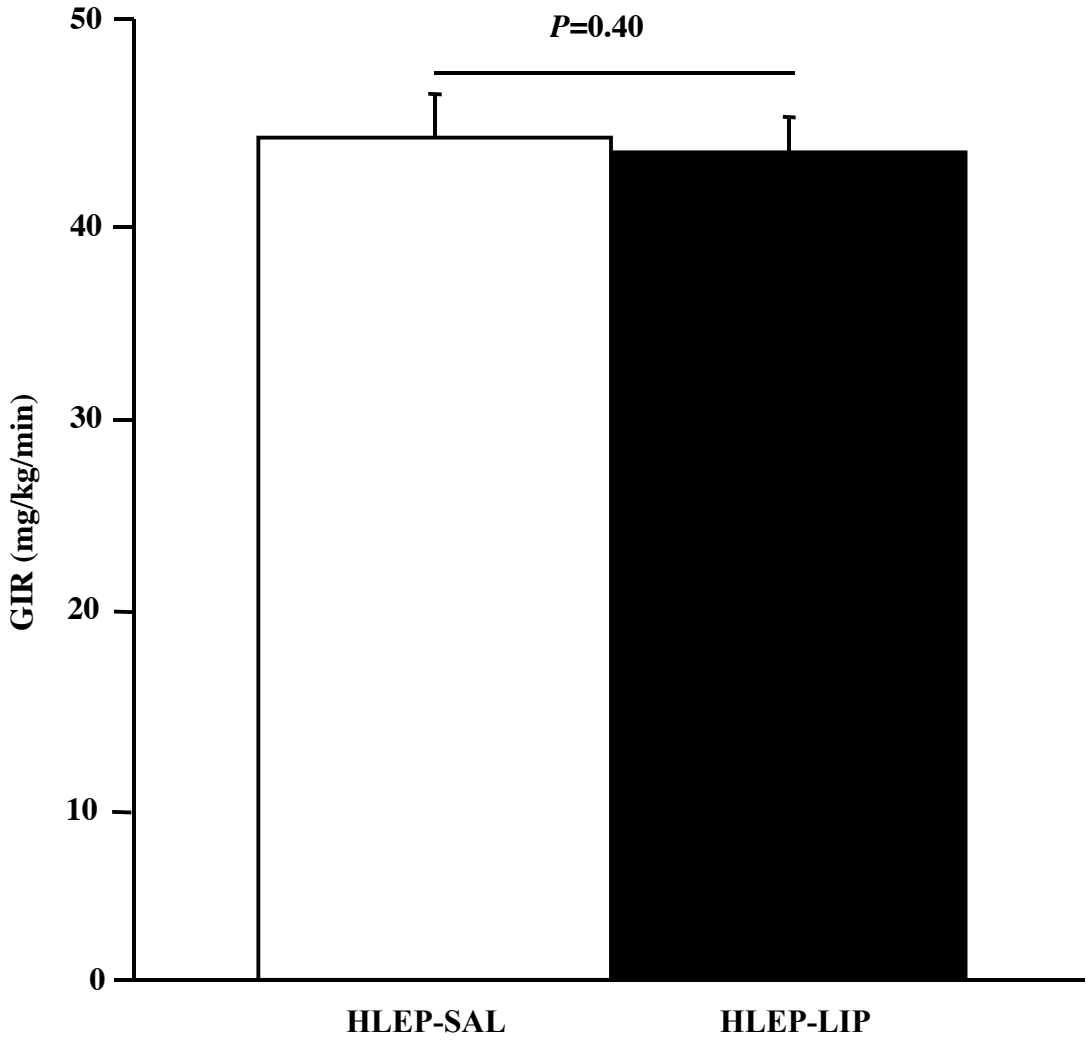

Fig. 17. ***Leptin prevents Intralipid induced insulin resistance.*** **Male Wistar rats were catheterized in the carotid artery and jugular vein, I.V. infused with adenovirus containing leptin cDNA (HLEP), and assigned to either 5h saline (HLEP-SAL) or lipid (HLEP-LIP) infusion as described in Methods. Insulin sensitivity was determined using a 90-minute hyperinsulinemic-euglycemic clamp. Glucose infusion rate (GIR) was averaged from the last 60-min of the clamp. Data are mean ± SEM; n=6/group.**

D. Leptin prevents Intralipid induced increases in skeletal muscle lipid content

Specific aim 3 was designed to explore the mechanisms involved in leptin-associated prevention of lipid induced SkM IR. We have demonstrated that leptin is able to prevent IR induced by lipid infusion (Fig. 17). This necessicitated the characterization of potential mechanisms associated with this novel finding. Previous investigations have established that IR elicited by acute hyperlipidemia is related to changes in SkM lipid content and in the IRS-1 signaling pathway via activation of second messengers which act to suppress cellular transduction of the insulin signal (i.e. PKCθ). Additionally, leptin has been linked to decreases in SkM lipid content, increases in fatty acid oxidation, and elevations in glucose uptake. We therefore assessed these parameters in our model of leptin prevention of lipid induced SkM insulin resistance.

The initial set of experiments examined the effect of leptin on SkM lipid accumulation (i.e. DAG, ceramide, and TG) following a 3h Intralipid infusion. As described in Methods, male Wistar rats were catheterized in the carotid artery and assigned to either an Intralipid (LIP, n=6) or saline (SAL, n=6) infusion protocol. Following recovery to presurgical body weight, rats were rendered hyperleptinemic (HLEP) by an IV infusion of adenovirus containing rat leptin cDNA. Food intake and body weight changes were monitored for 5d. Rats were fasted overnight and 3h LIP or SAL infusions were performed.

As demonstrated previously, 3h Intralipid infusion elicits significant increases in DAG and ceramide lipid levels (Fig. 14) in SOL. Lipid analysis of SOL from HLEP indicated no differences between HLEP-LIP and HLEP-SAL for DAG (2.5±0.2 vs 2.3±0.2 nMol/μg protein; P=0.21), ceramide (1.1±0.1 vs 1.0±0.1 nMol/μg protein; P=0.26), or TG (17.1±4.1 vs 16.0±2.6 μg/mg protein; P=0.42) following a 3h infusion (Fig. 18). These data

demonstrate that HLEP is able to (1) prevent deleterious increases of DAG and ceramide and (2) prevent alterations in TG content of SOL following a 3h lipid infusion.

In addition to SOL muscle tissue, a novelty of this project was the examination of SkM lipid content following leptin treatment in various fiber types, specifically, superficial vastus (VAS), predominately type 2-glycolytic fibers, and gastrocnemius (GAS), a mixed fiber type. Similar patterns in lipid content from VAS and GAS following leptin treatment were observed compared to SOL. Decreases in VAS DAG (0.6±0.1 vs 0.9±0.1 nMol/μg protein; *P*=0.01) and ceramide (0.8±0.2 vs 1.3±0.2 nMol/μg protein; *P*=0.06) in HLEP-LIP compared to HLEP-SAL were observed (Fig. 19). No differences were observed in TG (4.9±1.8 vs 5.3±0.8 μg/mg protein; *P*=0.43) in HLEP-LIP compared to HLEP-SAL (Fig. 19). No differences were observed in GAS DAG (1.2±0.1 vs 1.3±0.2 nMol/μg protein; *P*=0.25), ceramide (1.2±0.1 vs 1.5±0.2 nMol/μg protein; *P*=0.10), or TG (15.7±3.3 vs 16.0±2.8 μg/mg protein; *P*=0.47) in HLEP-LIP compared to HLEP-SAL (Fig. 20). These data demonstrate that leptin treatment is able to prevent increases in SkM lipid content following a 3h Intralipid infusion in various fiber types (i.e. type 2 and mixed).

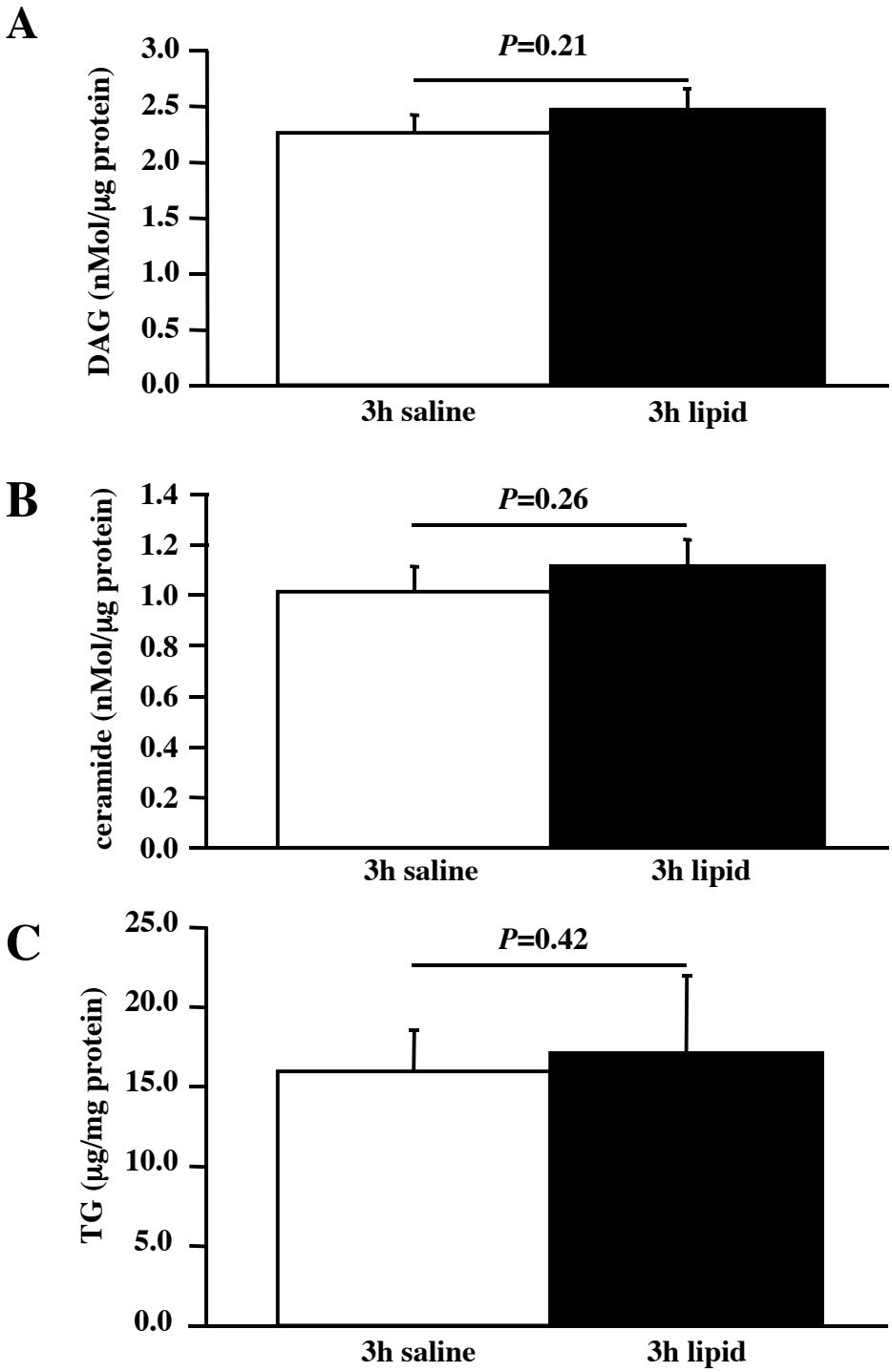

Fig. 18. ***Leptin prevents increases in soleus lipid content following Intralipid infusion.*** **Male Wistar rats were catheterized in the carotid artery and following recovery to presurgical body weight, administered an adenovirus containing rats leptin cDNA as described in Methods. Food intake and body weight changes were monitored for 5d and plasma FFA was elevated by a 3h Intralipid infusion. Skeletal muscle (A) DAG, (B) ceramide, and (C) TG content in soleus muscle was measured as described in Methods. Data are mean ± SEM; n=6/group.**

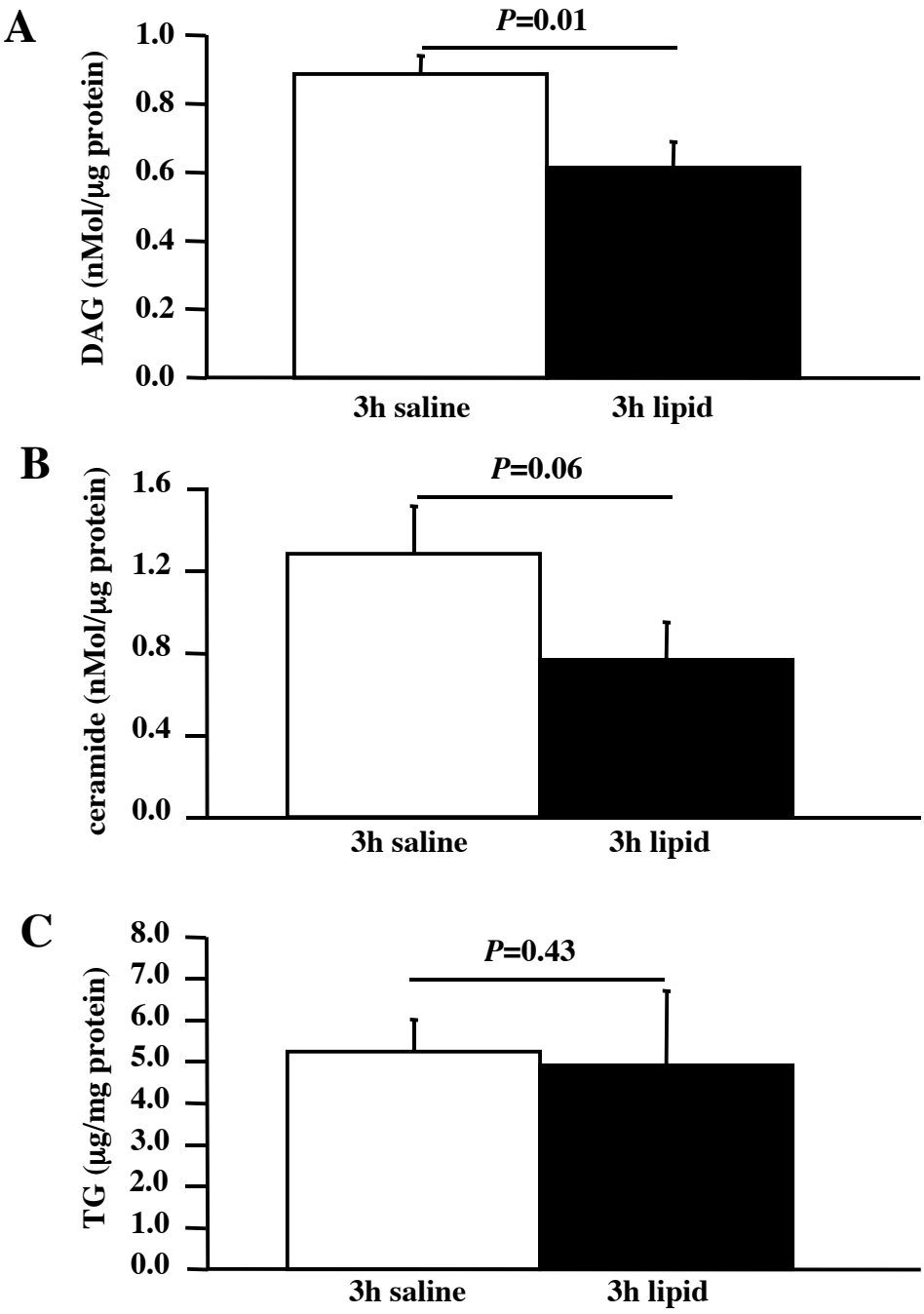

Fig. 19. ***Leptin prevents increases in superficial vastus lipid content following Intralipid infusion.*** **Leptin prevent Male Wistar rats were catheterized in the carotid artery and following recovery to presurgical body weight, administered an adenovirus containing rats leptin cDNA as described in Methods. Food intake and body weight changes were monitored for 5d and plasma FFA was elevated by a 3h Intralipid infusion. Skeletal muscle (A) DAG, (B) ceramide, and (C) TG content in superficial vastus muscle was measured as described in Methods. Data are mean ± SEM; n=6/group.**

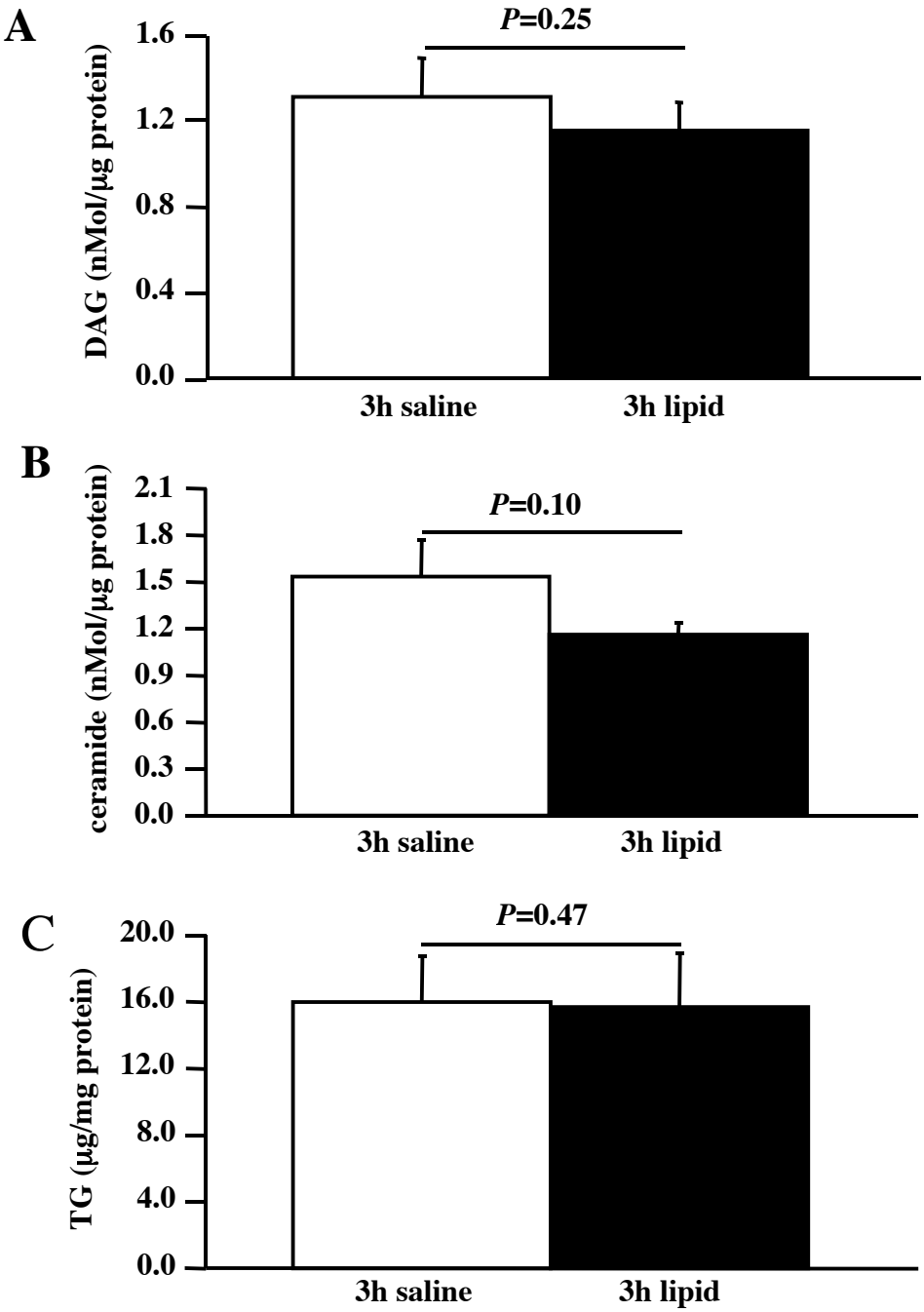

Fig. 20. ***Leptin prevents increases in gastrocnemius lipid content following Intralipid infusion.*** **Male Wistar rats were catheterized in the carotid artery and following recovery to presurgical body weight, administered an adenovirus containing rats leptin cDNA as described in Methods. Food intake and body weight changes were monitored for 5d and plasma FFA was elevated by a 3h Intralipid infusion. Skeletal muscle (A) DAG, (B) ceramide, and (C) TG content in gastrocnemius muscle was measured as described in Methods. Data are mean ± SEM; n=6/group.**

E. Fatty acid oxidation is not increased by leptin

Leptin prevents SkM lipid accumulation in all fiber types following 3h Intralipid infusion. One hypothesis proposed regarding the mechanism associated with the prevention of accumulated lipids is an increase in SkM fatty acid oxidation (FAox) with leptin treatment. The following results represent FAox measured in isolated SOL muscle from HLEP as described in Methods. No differences in FAox (2.8±0.4 vs 3.2±0.9 μMol palmitate/g tissue/h; P=0.76) between HLEP and controls (Fig. 21) were observed.

F. Fatty acid transporters are not decreased by leptin

Subsequent studies addressed perturbations in fatty acid transport into SkM. To control for the effects of adenovirus and the effects of leptin on food intake, control animals were administered an adenovirus containing the β-Galactosidase (βGal) cDNA gene (as described in Methods) and were calorically matched to hyperleptinemic animals throughout the treatment protocol (5d). Following an overnight fast, βGal treated animals were infused for either 3h or 6h with Intralipid (LIP) or saline (SAL), anesthetized with ~70 mg/kg Nembutal, and tissues quickly excised and frozen in liquid nitrogen for later analysis. Due to the high quantity of tissue required for plasma-membrane fatty acid binding protein (FABPpm) and fatty acid transporter (FAT/CD36) analysis, only gastrocnemius tissue was assessed. Dr. Arend Bonen at the University of Guelph, Ontario, CA kindly provided the analysis of FABPpm and FAT/CD36 from 3h HLEP-SAL and βGal-SAL. No differences between HLEP-SAL and βGal-SAL were evident in either FABPpm or FAT/CD36 (Fig. 22).

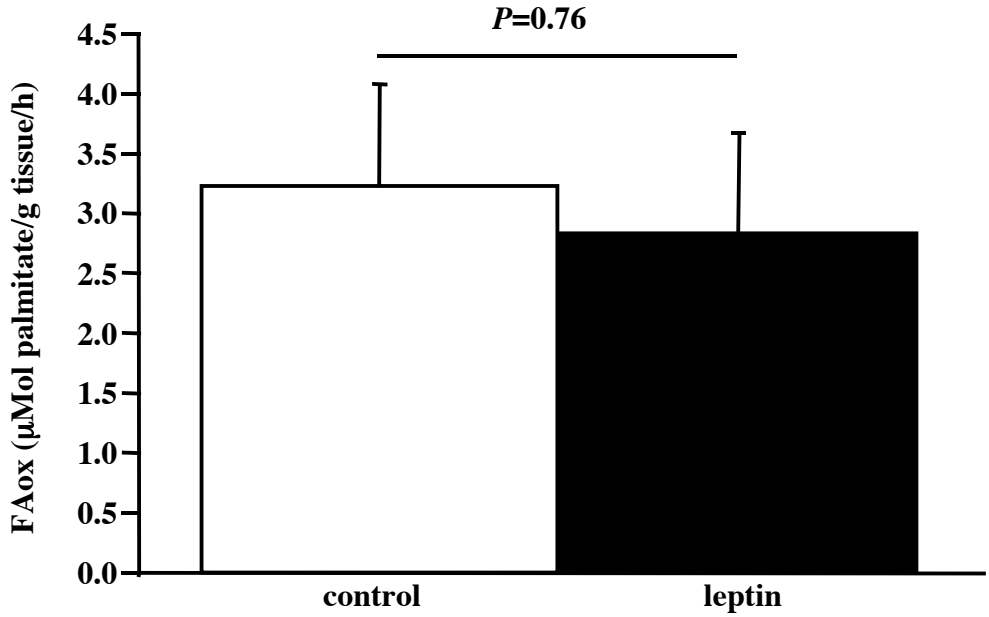

Fig. 21. ***Fatty acid oxidation of isolated leptin treated soleus muscle.*** **Male Wistar rats were rendered hyperleptinemic by administration of an adenovirus containing rat leptin cDNA via tail vein injection as described in Methods. Controls received no virus. Animals were monitored for food intake and body weight changes for 5d. Following an overnight fast, rats were anesthetized under isoflurane and soleus muscles quickly excised. Muscles were equilibrated in KRH buffer for 20 minutes and then moved to KRH containing ^{3}H-palmitate for 60 minutes. Rates of fatty acid oxidation (FAox) were calculated as described in Methods. Values are mean SEM; n=3/group.**

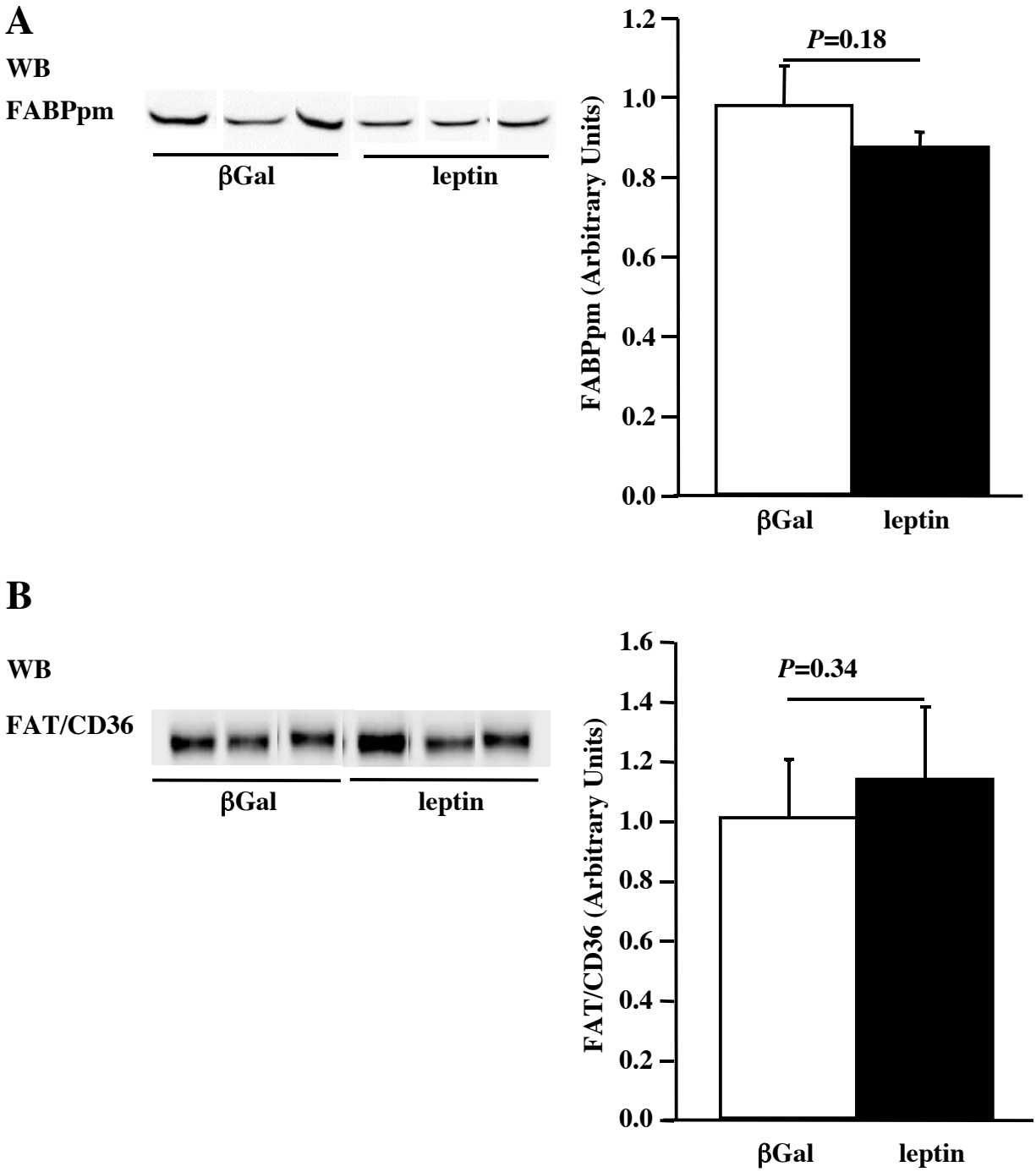

Fig. 22. ***Fatty acid transporters following leptin treatment.*** **Male Wistar rats were catheterized in the carotid artery and administered an adenovirus containing either leptin or β-Galactosidase (βGal) as described in Methods. Food intake and body weight changes were monitored for 5d, βGal were calorically matched to leptin. Following an overnight fast, rats were infused for 3h with saline. Proteins for (A) fatty acid binding protein (FABPpm) and (B) fatty acid transporters (FAT/CD36) were measured in gastrocnemius muscle as described in Methods. Representative immunoblot images are shown. Data are mean ± SEM; n=6/group.**

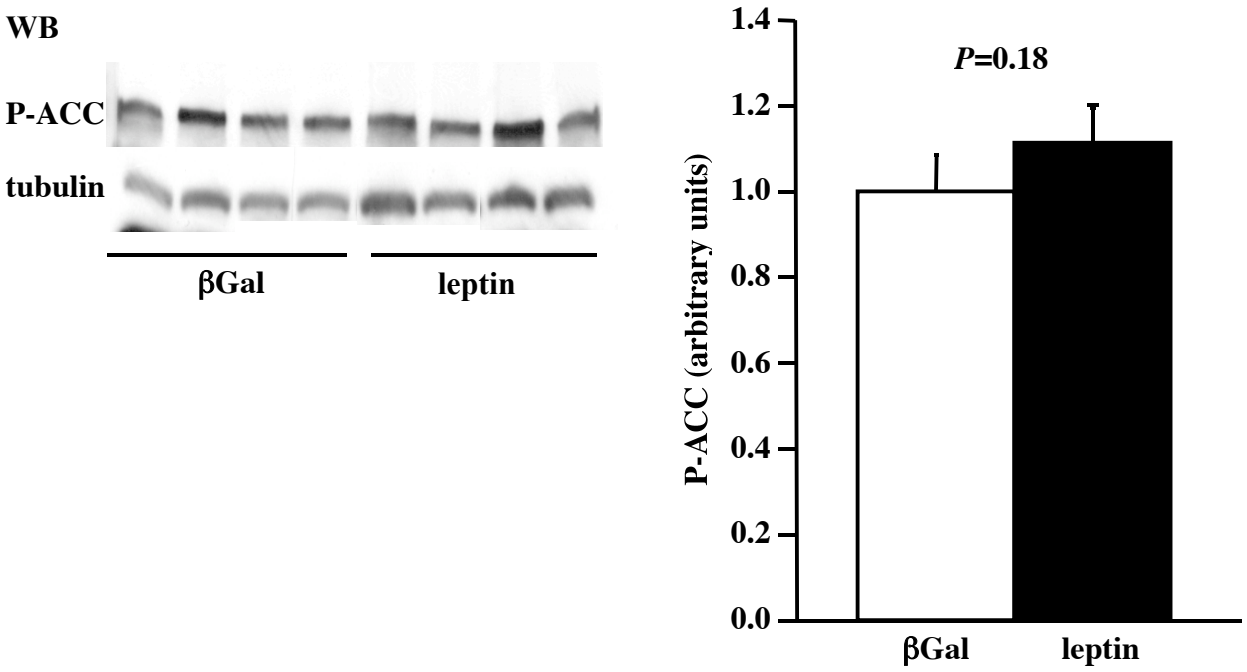

Fig. 23. ***P-ACC in soleus muscle following leptin treatment.*** **Male Wistar rats were catheterized in the carotid artery and administered an adenovirus containing either leptin or β-Galactosidase (βGal) as described in Methods. Rats were infused for either 3h or 6h with Intralipid. Controls received a saline infusion. Proteins for phosphorylated acetyl-CoA carboxylase (P-ACC) content in soleus muscle were analyzed by western blot analysis. Data from 3h and 6h were combined for final analysis. Representative immunoblot images are shown. Data are mean ± SEM; n=12/group.**

G. Phosphorylated acetyl-CoA carboxylase protein content in soleus is not changed by leptin

It was hypothesized that leptin may be altering mechanisms regulating FAox through allosteric regulation of acetyl-CoA carboxylase (P-ACC) and intracellular formation of Malonyl-CoA, a potent regulator of FAox. However, basal (HLEP-SAL vs βGal-SAL) vs lipid challenge (HLEP-LIP vs βGal-LIP) P-ACC in SOL was not different. When the data were combined (i.e. HLEP-SAL and HLEP-LIP vs βGal-SAL and βGal-LIP), P-ACC was decreased (0.9±0.3 vs 1.8±0.5 arbitrary units (AU); P=0.07) in HLEP compared to βGal following a 3h infusion, although not statistically so. Finally, no differences in P-ACC were observed between HLEP and βGal following 6h Intralipid. Therefore, the data were combined in Fig. 23.

H. Metabolic gene expression is changed with leptin

Gene expression changes in response to leptin treatment were hypothesized to contribute to improvements in insulin action following Intralipid infusion. Several gene transcripts including Sterol Regulator Element Binding Protein 1c (SREBP-1c), a regulator of fatty acid synthesis, Uncoupling Protein-3 (UCP), involved in glucose uptake, and Acetyl CoA Carboxylase-2 (ACC2), an allosteric regulator of Malonyl CoA and fatty acid oxidation were of particular interest. SOL muscle RNA was isolated from βGal or leptin adenovirus treated male Wistar rats infused for 3h with saline. Genes were amplified by RT-PCR as described in Methods. SREBP-1c expression (Fig. 24A) was significantly increased with leptin treated compared to βGal (2.2±0.1 vs 1.7±0.2 Arbitrary Units, P=0.04), indicating enhanced regulation of fatty acid synthesis genes in soleus muscle. In contrast, UCP3 (Fig. 24B) expression was unchanged in response to leptin (3.1±0.3 vs 2.8±0.6 Arbitrary Units, P=0.33)

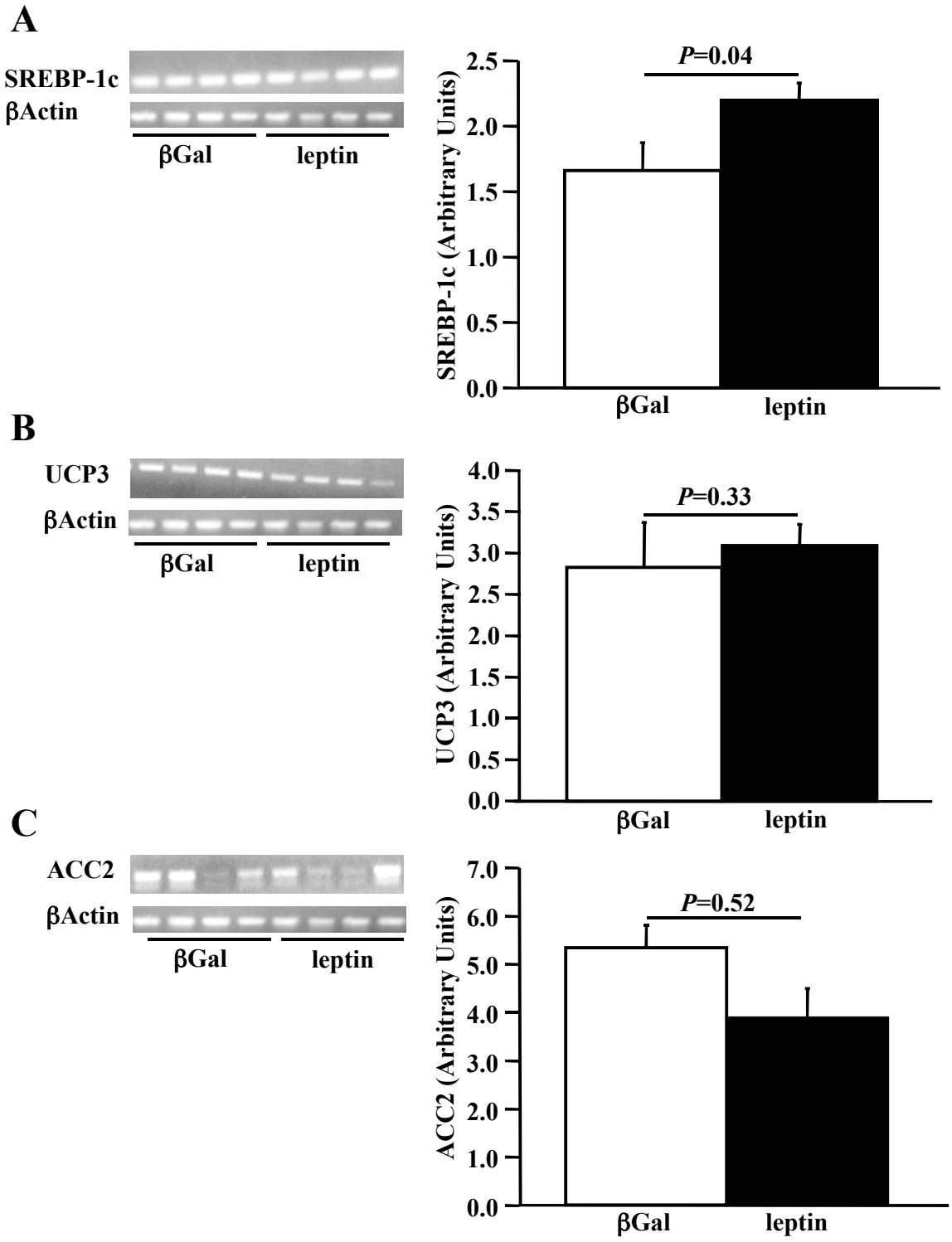

Fig. 24. ***Alterations of expression in selected metabolic genes.*** **Gene expression of (A) SREBP-1c, (B) UCP3, and (C) ACC2 were measured by RT-PCR in soleus muscle. Male Wistar rats were administered an adenovirus containing either β-Galactosidase (βGal) or leptin cDNA and infused with saline for 3h. Representative images of PCR generated from soleus muscle cDNA are shown. Values are mean ± SEM; n=4/group.**

compared to βGal, demonstrating that increased glucose uptake is not correlated to an increase in gene expression. Finally, ACC2 (Fig. 24C) expression in soleus was significantly lower (3.9±0.6 vs 5.4±0.5 Arbitrary Units, *P*=0.05) in leptin compared to βGal, suggesting a decrease in Malonyl CoA production and subsequent increase in fatty acid oxidation paralleling observations in SkM lipid content following leptin treatment.

I. PKCθ protein content is decreased by leptin

It has been demonstrated that elevated SkM lipids, specifically DAG and ceramide, lead to the activation of classic and novel PKC isoforms, and activation of PKCθ in particular appears to be causative of the deleterious effects of lipid exposure on the insulin-signaling pathway (59). Therefore, fractionation studies of PKCθ (cytosolic and membrane) from rats administered either an adenovirus containing leptin (HLEP) or βGal and infused for 6h with Intralipid (LIP) as described in Methods. Results indicate significant decreases in cytosolic-associated (0.7±0.1 vs 1.0±0.1 arbitrary units; *P*=0.003) and membrane-associated PKCθ (0.7±0.1 vs 1.0±0.1 arbitrary units; *P*=0.01) in 6h HLEP-LIP compared to βGal-LIP (Fig. 25A, 25B). Finally, calculated total PKCθ (membrane + cytosolic fractions) indicated significant decrease (1.5±0.2 vs 2.0±0.1 arbitrary units; *P*=0.02) for HLEP-LIP compared to βGal-LIP (Fig. 25C).

A subsequent study was conducted to address the effect of HLEP *per se* on PKCθ. No significant differences in membrane, cytosolic, or calculated total PKCθ expression in SOL from HLEP and βGal (Fig. 26A-C) were observed. These data suggest that leptin *per se* does not alter the basal expression of PKCθ.

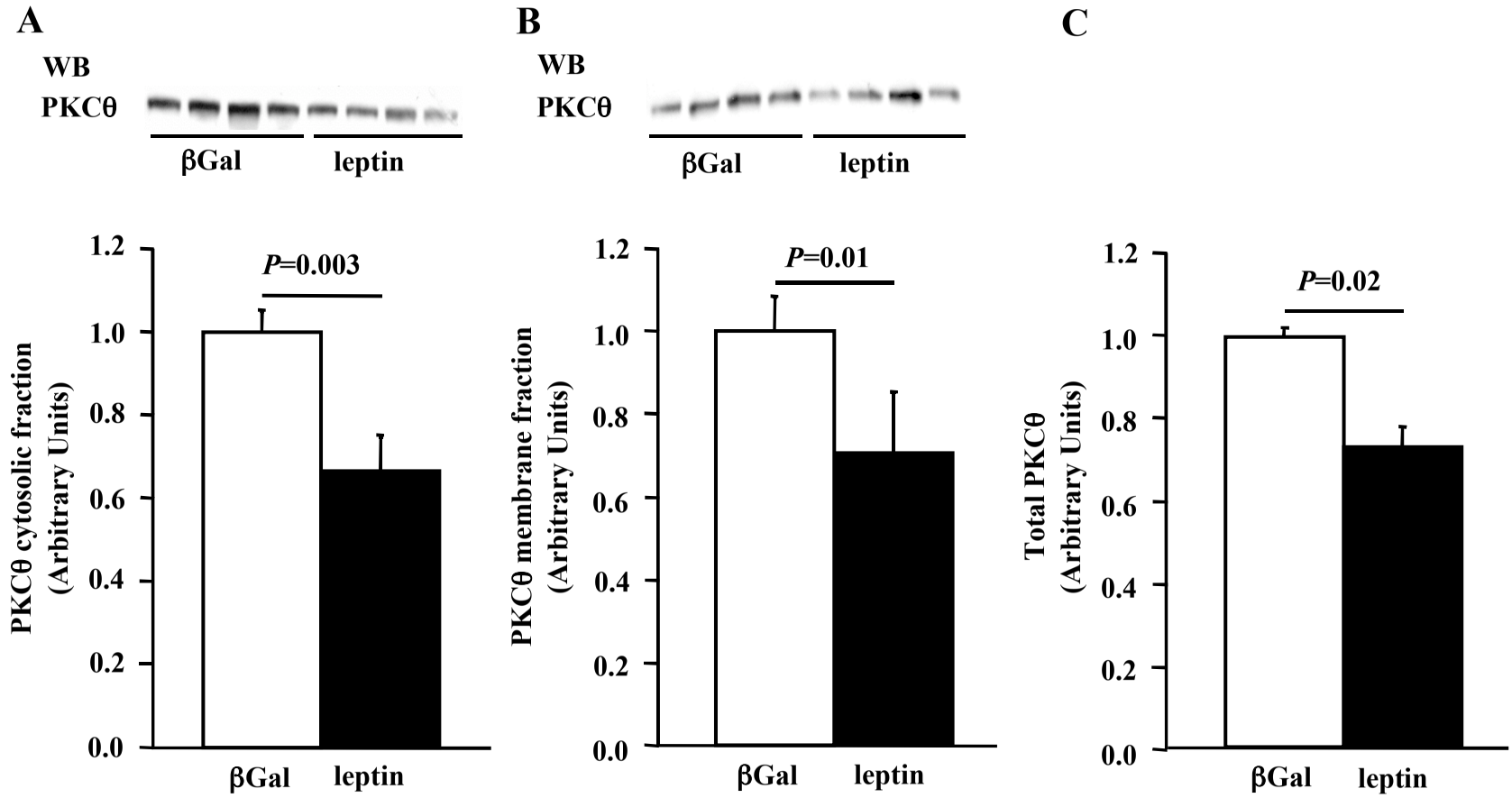

Fig. 25. ***Effects of leptin on PKCθ fractions following 6h Intralipid.*** **Male Wistar rats were catheterized in the carotid artery and administered an adenovirus containing either β-Galactosidase (βGal) or leptin. Leptin animals were monitored for 5d for food intake and body weight changes, βGals were calorically matched to leptin animals. Following an overnight fast, rats were infused for 6h with Intralipid as described in Methods. Animals were anesthetized, tissues quickly excised, and frozen in liquid nitrogen or later analysis. Proteins for PKCθ cytosolic and membrane fractions were analyzed by Western blot analysis as described in Methods. Total PKCθ was calculated by added the cytosolic and membrane fractions. Representative immnoblots are presented. Data are mean ± SEM, n=6/group.**

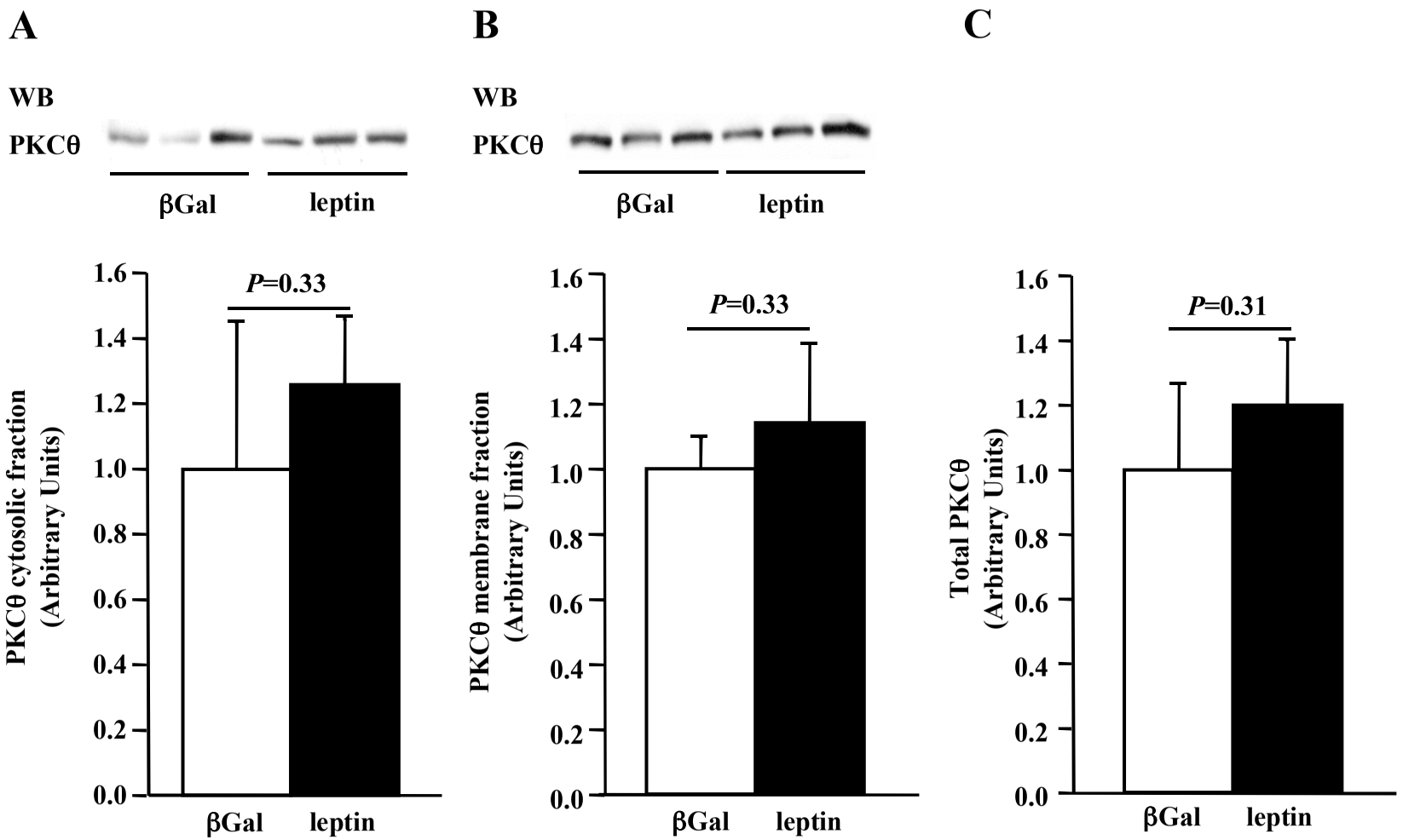

Fig. 26. ***Effects of leptin per se on PKCθ fractions.*** **Male Wistar rats were catheterized in the carotid artery and administered an adenovirus containing either β-Galactosidase (βGal) or leptin. Leptin animals were monitored for 5d for food intake and body weight changes, βGals were calorically matched to leptin animals. Following an overnight fast, rats were anesthetized, tissues quickly excised, and frozen in liquid nitrogen or later analysis. Proteins for PKCθ cytosolic and membrane fractions were analyzed by Western blot analysis as described in Methods. Total PKCθ was calculated by added the cytosolic and membrane fractions. Representative immnoblots are presented. Data are mean ± SEM, n=6/group.**

J. Leptin does not prevent insulin resistance induced by hindlimb denervation

The final arm of the project addressed the role of leptin in the prevention of IR in a different model system, specifically hindlimb denervation. Denervation of skeletal muscle elicits IR (55, 60) and the mechanisms contributing to with this phenomenon are poorly understood. However, it has been demonstrated that denervated SkM has impaired insulin-stimulated glucose uptake and that it may be associated with increased levels of SkM lipid content (i.e. DAG and ceramide). As demonstrated previously, these lipids contribute to deleterious affects on the insulin-signaling cascade. Initial studies were designed to establish IR following hindlimb denervation. The sciatic nerve from male Wistar rats was denervated as described in Methods and monitored for 72h. Following an overnight fast, rats were anesthetized, SOL muscles quickly excised and glucose uptake measured. As demonstrated in Fig. 27, insulin stimulation elicited a 2-fold increase in glucose uptake from control animals. In contrast, no increase in insulin stimulated glucose uptake was observed in the denervated muscle.

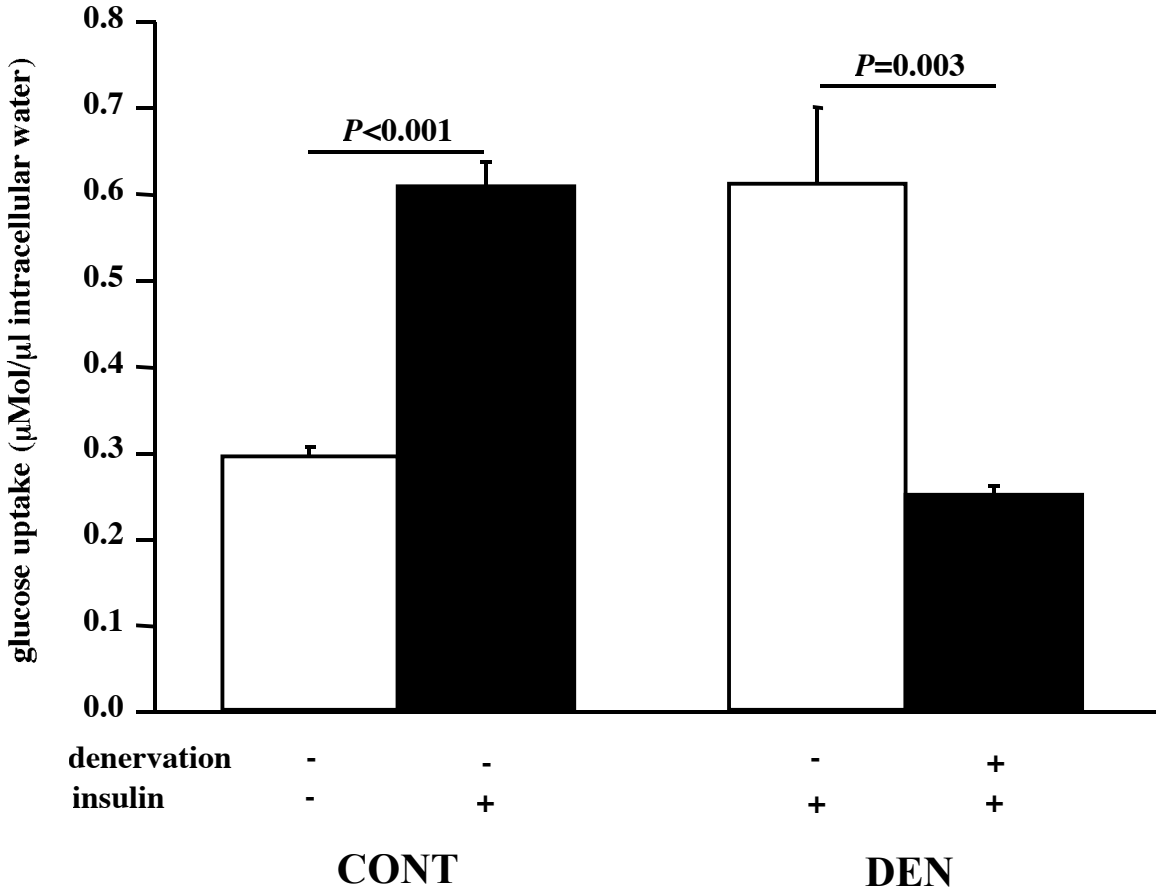

Fig. 27. ***Glucose uptake in denervated soleus muscle.*** **The sciatic nerve from male Wistar rats was exposed through blunt dissection and excised (DEN) and monitored for 72h as described in Methods. Control (CONT) rats did not undergo surgery. Following an overnight fast, rats were anesthetized, soleus muscles quickly excised and glucose uptake measured. Data are mean ± SEM, n=4 muscles/group.**

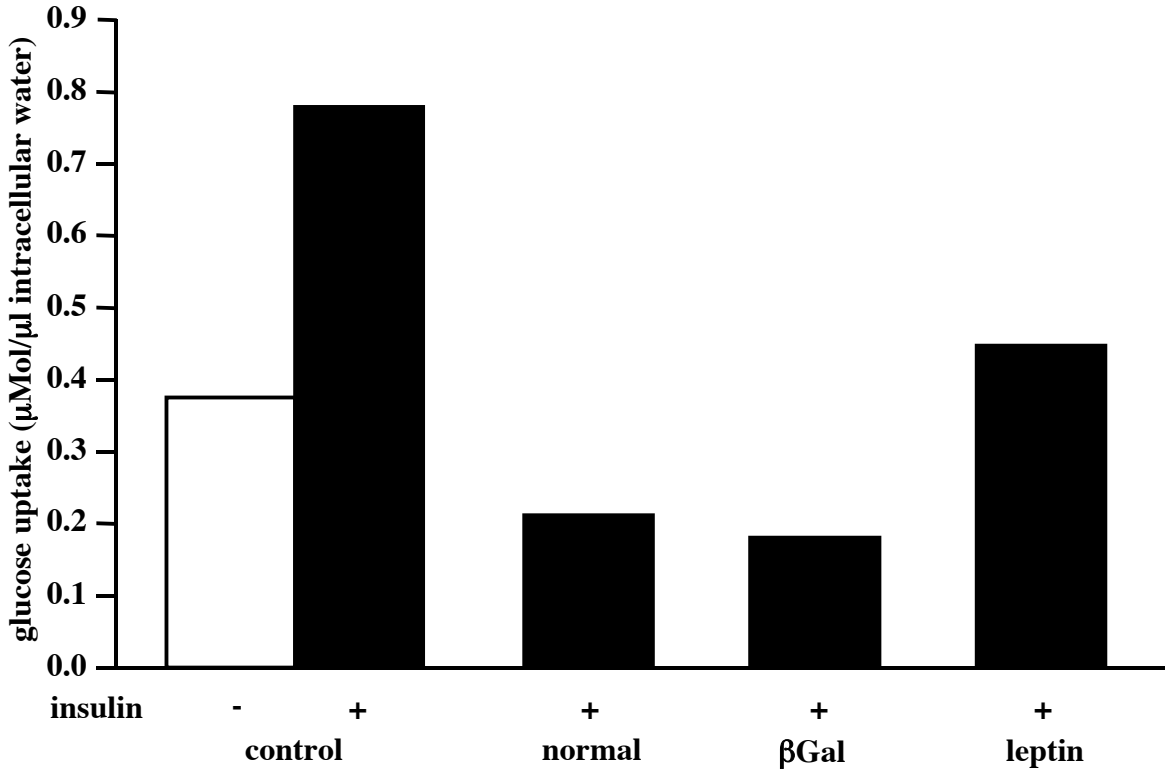

Fig. 28. ***Glucose uptake from leptin treated denervated muscle.*** **Male Wistar rats were administered an adenovirus containing either β-Galactosidase or leptin through tail vein injections as described in Methods. Forty-eight hours later, the sciatic nerve was exposed and excised. Rats were monitored for 72h for food intake and body weight changes. Following an overnight fast, rats were anesthetized, soleus muscle quickly excised and glucose uptake measured as described in Methods. Data are mean of 2 muscles/group.**

As demonstrated previously insulin stimulation elicits an approximate 2-fold increase in glucose uptake in isolated SkM. However, insulin has no effect on glucose uptake in denervated muscle. Additionally, insulin stimulation had no effect of glucose uptake from βGal treated denervated muscle. Finally, glucose uptake in insulin stimulated denervated muscle following leptin treatment was moderately, if at all, increased compared to normal and βGal treated denervated muscle (Fig. 28). It should be noted that the results are means from only two muscles. Further, there were significant variances in the response from leptin treated animals; therefore caution must be taken in interpretation.

VI. Discussion

A. Overview

Type II diabetes is now considered a worldwide epidemic. Associated with the disease are hyperinsulinemia and hyperglycemia owing to the development of IR. The mechanisms associated with the development of IR are incompletely understood, however, excess energy supply is suggested to be a key player in the condition. Specifically, excess energy in the form of lipid is of particular interest due to the relatively high content in the Western diet and subsequent increasing cases of Type 2 diabetes. Lipid oversupply in the form of either chronic high fat feeding or acute lipid infusion elicits deleterious results in SkM, an important site of glucose uptake. These results include, but are not limited to, increases in SkM lipid content, increases in cytokine signaling, and disruptions in the insulin signal cascade (Review in (47)). The adipocyte derived hormone leptin, while first thought to be an antiobesity agent, has been demonstrated to play complex role in insulin action. Leptin treatment has been shown to improve SkM fatty acid metabolism and glucose uptake in several models of IR (2, 7, 36, 52). Reports have demonstrated the ability of leptin to reverse

SkM IR following high fat feeding (7) and in genetic models of obesity (39). However, no studies have directly addressed the ability of leptin to prevent lipid induced IR.

This project addressed the ability of leptin to prevent IR in two *in vivo* different models. Specifically, the acute hyperlipidemia (Intralipid) and hindlimb denervation models of IR. Initial studies were designed to confirm the IR phenotype following Intralipid. Principle results from the initial studies were (1) 5h Intralipid induces IR and (2) SkM lipid content is increased following 3h Intralipid. Subsequent studies from rats rendered hyperleptinemic by adenovirus administration followed by Intralipid addressed the ability of leptin to prevent IR and examined the mechanisms associated with the prevention. Principle results from these studies were: (1) leptin is able to prevent IR induced by Intralipid, (2) leptin prevents increases in SkM lipids (DAG and ceramide) following 3h Intralipid, (3) improvements in insulin sensitivity may not be associated with increased fatty acid oxidation, decreases in fatty acid transporters, or alterations in P-ACC, and (4) leptin may prevent IR elicited by Intralipid by inhibiting the activation of PKCθ.

B. Intralipid induced insulin resistance

Previous reports from human and animal studies have demonstrated that exogenous lipid infusion elicits SkM IR (24, 31, 59). This method is useful because (1) the development of IR occurs in a relatively short time period (3-5h), (2) the plasma lipid profile is similar to obesity models of IR, and (3) the lipid infusion is the sole mechanism for leading to the development of IR. Additionally, the deficits in insulin signaling in response to Intralipid are transient. Yu and colleagues (59) reported significant decreases in IRS-1 tyrosine phosphorylation and IRS-1-associated PI3-kinase activity in response to a 5h lipid infusion. However, following a washout period, values returned to baseline demonstrating a reversal of

the deleterious effects associated with lipid infusion. Here, using hyperinsulinemic-euglycemic clamps, we demonstrate IR following a 5h Intralipid infusion (Fig. 13). The demonstration of this observation is important because it establishes the framework for later studies involving leptin treatment. Subsequent studies were designed to examine SkM lipid content following both a 3h and 6h Intralipid infusion.

C. Intralipid induced increases in skeletal muscle lipid content

Three-hour lipid infusion, but not 6h, elevates lipid species DAG and ceramide in SOL. Previous reports from animal models have demonstrated increases in the lipid species DAG and ceramide in SOL in as little as 3h of a lipid infusion (59). Further, the authors report significant decreases in TG content following a 3h lipid infusion. The current study corroborates the reported observations with respect to SkM DAG, ceramide, and TG content following a 3h Intralipid infusion. The mechanism associated with the observed decrease in TG from SOL may be related to the increase in intracellular fatty acyl-CoA by Intralipid. As suggested by others (59), the increase in intracellular fatty acyl-CoA may activate a phospholipase that leads to an increase in DAG from endogenous lipid sources. In contrast, we report sustained increases in SOL ceramide content following a 6h Intralipid infusion. The sustained elevation of ceramide content at 6h suggests the development of SkM "lipotoxicity" in that the inflexibility of SkM to respond to constant lipid oversupply leads to chronic elevation of ceramide.

It is recognized that the increases in DAG and ceramide following the 3h Intralipid reported here are not as dramatic as demonstrated by others using a similar model (59). However, it should be noted that there were significant differences in the lipid analysis method between the two studies. In our study, DAG and ceramide were separated by the

TLC method, however, Yu and colleagues (59) used liquid chromatography tandem mass spectroscopy (LCMS/MS). The benefit of the LCMS/MS methods is that it provides for a quantification of individual DAG species. As reported by Yu *et al.*, all DAG species are increased by Intralipid, however, it is unknown if all species contribute to Intralipid induced IR equally. While the LCMS/MS technology was unavailable for the current investigation; the TLC method is reliable in that intra-assay and inter-assay variability was low (<6%, data not shown). It is apparent that in spite of the relatively small increases in SkM lipid content (DAG and ceramide) the phenotype of IR remained.

No reports have provided a comprehensive fiber type analysis of the effects of acute hyperlipidemia. This study provides evidence that accumulation of lipid in SkM by lipid oversupply is not fiber type specific. Several reports demonstrate that exogenous lipid oversupply elicits inappropriate accumulation of lipids and subsequent IR in SOL due to the high insulin responsiveness of the tissue (24, 59). The current data set expands this observation to include other fiber types that are also insulin responsive. Significant increases in both DAG and ceramide were observed in both VAS and GAS following a 3h lipid infusion (Figs. 15 and 16). These data demonstrate that all SkM is subjected to inappropriate accumulation of lipid. Therefore, it is reasonable to suggest that lipid accumulation in these fiber types contributes to deleterious effects of insulin action resulting in the development of IR.

D. Leptin prevents insulin resistance induced by Intralipid

The adipocyte derived hormone leptin has been established as an important regulator of food intake in rodents (28). However, of particular interest is the role of leptin in energy metabolism. Several *in vivo* studies demonstrate that leptin treatment can reverse IR induced

by high-fat feeding (7) or genetic predisposition (39). The putative mechanisms associated with improvements in SkM insulin sensitivity by leptin include decreases in lipid content (7), increases in lipid metabolism (52), and decreases in fatty acid transport (5). However, no studies have directly assessed the capacity of leptin to improve IR through action on lipid metabolism. Therefore, a series of studies were designed to examine if leptin could prevent IR induced by Intralipid. Rats were rendered HLEP by the administration of an adenovirus containing leptin cDNA. This method was chosen because it allows for elevation of plasma leptin concentration in a minimally invasive manner. Insulin sensitivity of the HLEP rats was measured by hyperinsulinemic-euglycemic clamp method following a 5h Intralipid infusion. The results indicate no difference in glucose infusion rate compared to saline controls (Fig. 17). These data confirm the hypothesis that leptin can prevent Intralipid induced IR. To explain these observations, several mechanisms were explored including the examination of SkM lipid content, fatty acid metabolism, and activation of membrane associated PKCθ.

E. Leptin prevents increases in skeletal muscle lipid content induced by Intralipid

As stated previously, increases in SkM lipid content are associated with the development of IR. The administration of leptin to high-fat fed rats elicits a significant decrease in SkM TG content (7, 52). Therefore, the initial hypothesis for the prevention of lipid induced IR by leptin related to the prevention of increases in SkM DAG, ceramide, and TG content induced by Intralipid (Figs. 14-16). Lipid analysis from HLEP SOL following 3h Intralipid indicated no differences in DAG, ceramide and TG content compared to saline (Fig. 18). These data demonstrate that in spite of the increase in plasma FFA, lipid does not accumulate in leptin treated SkM. Previous reports have focused on effects of leptin on SOL (7, 51), however, the

current study examined lipid content from all SkM fiber types. As demonstrated previously, Intralipid increases lipid content in VAS and GAS indicating lipid accumulation of lipid is not fiber type specific. Given the observation from SOL, the working hypothesis was that leptin would prevent lipid accumulation in VAS and GAS. No increases in SkM lipid content were observed in VAS or GAS from HLEP rats following 3h Intralipid infusion (Figs. 19 and 20). These data demonstrate that the effects of leptin are not fiber type specific suggesting that the proposed mechanisms for improvements on insulin action (i.e. increases in fatty acid oxidation) may be applicable to all SkM fiber types.

One interesting observation was that DAG is significantly decreased in VAS following lipid infusion. Based on previous reports of increased SOL (type I fibers) and isolated EDL (type II fibers) mice muscles (50) oxidative capacity following leptin treatment, it could be hypothesized that in the rat, type II-glyolytic fibers, develop an enhanced ability to oxidize fat in response to leptin treatment. Further, exposure to exogenous lipid may trigger an increase in endogenous lipid oxidation and subsequent depletion of DAG. While these results are intriguing, the potential mechanism was not explored because it did not fit the specific aims of the study.

F. Mechanisms associated with the prevention of Intralipid induced insulin resistance by leptin

It has been demonstrated that Intralipid infusion elicits increases in SkM lipid content and the increases are associated with decreased levels of FAox (32), increases in FAT/CD36 and FABPpm (6), and activation of PKCθ (24). Taken together, these alterations in SkM lipid content and deleterious effects on the insulin-signaling cascade contribute to the development of IR. Here we report that leptin administration prevents increases in SkM lipid content by

Intralipid infusion. Therefore, several mechanisms including FAox, fatty acid transporters, metabolic gene expression, and PKCθ activation were assessed to elucidate how leptin prevents Intralipid induced IR.

As stated previously, leptin is known to increase FAox in SkM (5, 52). Therefore, FAox was measured directly from isolated SkM. Results from isolated SkM indicated no difference in FAox between HLEP and normal controls (Fig. 21) in corroboration with previous reports (52). As hypothesized by others (52), the ability to measure increases in FAox from isolated SkM may require an increase in metabolic demand (i.e. contraction). Moreover, it may be necessary to evaluate increased FAox by leptin using whole-body methods. In contrast, increased FAox from isolated muscle in the presence of leptin has been reported in *ob/ob* mice compared to controls (36). The fundamental difference between the two methods is that the *ob/ob* mouse lacks functional leptin, whereas in the adenovirus model leptin levels have been increased from normal-physiologic to supra-physiologic. Therefore, it is reasonable to suggest that muscles with no prior exposure to leptin are more likely to respond than those with previous exposure.

Transport of FA into SkM is primarily regulated by FAT/CD36 and FABPpm. Additionally, these proteins themselves are regulated by diet, exercise, and insulin (Review in (45)). Due to the observation that FAox is not increased in isolated muscle following chronic HLEP and previous studies demonstrating decreases in both FABPpm and FAT/CD36 following leptin treatment (51) another hypothesis was proposed. Specifically, that the mechanism associated with a prevention of SkM lipid accumulation following Intralipid by HLEP was related to decreases in FA binding and transport into SkM. To address this hypothesis, whole muscle homogenates from HLEP and βGal treated GAS were

sent to Dr. Arend Bonen, University of Guelph, for analysis. Gastrocnemius tissue was used in the current experiment due to the lack of available SOL tissue. Further, it was hypothesized that the effects of leptin observed in SOL (5) would hold true for GAS. However, no significant differences were observed between the groups for FABPpm and FAT/CD36 protein content (Fig. 22). Therefore, in a mixed fiber type, the role of leptin my not be as robust as seen in other fiber types.

As demonstrated previously, FAox, FAT/CD36 and FABPpm were unchanged in response to leptin treatment in the current study. It was hypothesized that P-ACC may be increased as an indirect measure of improved FAox. Specifically, an observed increase in P-ACC following Intralipid would indicate a decrease in Malonyl CoA production and subsequent increase FAox. Therefore, indirect measures of FAox included the analysis of P-ACC from HLEP and βGal whole muscle homogenates. As demonstrated previously, no differences HLEP and βGal in SOL in any infusion condition, therefore, the data were combined for a final analysis (Fig. 23). These data demonstrate that alterations in P-ACC cannot be detected following chronic leptin treatment in SOL. It is possible that the analysis of P-ACC occurred at a time other than when differences were present. That is to say that alterations in P-ACC following HLEP occur earlier in the treatment period. Therefore, by measuring P-ACC at Day 6 of the treatment period following an overnight fast, differences are missed. Therefore, an analysis of leptin or βGal treated rats in the fed state may provide insight into mechanisms regulating FAox.

Due to the negative data generated from the analysis of FAox, FAT/CD36 and FABPpm, and P-ACC, it was of interest to examine gene expression related to fatty acid synthesis, glucose uptake, and regulators of fatty acid oxidation. Using RT-PCR, SREBP-1c, UCP3,

and ACC2 were examined. Significant increases in SREBP-1c expression were observed with leptin treatment compared to βGal in SOL muscle (Fig. 24A). Increases in SREBP-1c expression are associated with increases in fatty acid synthesis. In refeeding studies, leptin treatment decreased SREBP-1c expression, however, protein levels were not different from controls. It is difficult to interpret the current observed changes in SREBP-1c expression due to the nutritional status (i.e. fasting) of the animal. However, it could be hypothesized that leptin may tightly regulate oscillations of SREBP-1c expression within SkM. Whereas under normal physiologic conditions SREBP-1c is decreased in the fasting state and increased during refeeding, leptin may maintain expression at a relative constant throughout various nutritional states.

As demonstrated previously, leptin treatment increases glucose uptake (7). Therefore, UCP3 was analyzed due to its role in SkM glucose metabolism. No differences were observed between βGal and leptin treated animals, suggesting the increases observed in glucose uptake are not related to UCP3 gene expression (Fig. 24B). In contrast, ACC2 expression was significantly decreased following leptin treatment compared to βGal (Fig. 24C). ACC2 is an allosteric regulator of fatty acid oxidation. Decreases in ACC2 expression suggest a decrease in Malonyl CoA formation and an increase in fatty acid oxidation. These data are in agreement with the observations of SkM lipid content following leptin treatment.

The activation of membrane associated PKCθ is correlated with lipid induced SkM IR (47, 59). Activation of PKCθ is in response to increased SkM lipid levels, specifically, DAG. It has been demonstrated that HLEP prevents accumulation of DAG following Intralipid (Fig. 14-16). As such, it was hypothesized that HELP would prevent the activation of membrane-associated PKCθ in response to Intralipid. Fractionation studies were

completed to address the affect HLEP on membrane and cytosolic associated PKCθ following a lipid infusion. Cytosolic and membrane fraction of PKCθ were significantly decreased following a 6h lipid infusion in leptin compared to βGal treatment (Fig. 25). Calculation of total PKCθ (cytosolic + membrane fraction) indicated HLEP-LIP was significantly lower compared to βGal-LIP. Together, these data suggest that when posed with a lipid challenge, HLEP prevents increases in total, cytosolic, and membrane associated PKCθ. In contrast, basal protein expression of PKCθ is unchanged with leptin treatment (Fig. 26). These data are supported by evidence from PKCθ knockout mice that demonstrated increased glucose uptake and IRS-1 tyrosine phosphorylation following a lipid infusion when compared to controls (33). Therefore, leptin serves as a protective mechanism by preventing increases in membrane-associated PKCθ translocation following acute hyperlipidemia.

The observation that PKCθ membrane and cytosolic fraction are decreased in response to a lipid challenge without a decrease in basal expression is puzzling. It is established that lipids, specifically DAG, regulate the activation of PKCθ (47). Data presented here demonstrate that in response to a lipid challenge DAG does not change in HLEP SOL. Following the observation that DAG levels regulate PKCθ levels, one would expect PKCθ levels to remain unchanged following Intralipid infusion. However, downregulation in response to a lipid challenge may indicate that there are additional factors that regulate activation of PKCθ. Potential mechanisms related to regulation of PKCθ in response to lipid oversupply include an increase SkM oxidation, upregulation of oxidative gene expression, or alterations in substrate cycling. Future studies are required to elucidate this issue.

G. Leptin does not prevent insulin resistance induced by hindlimb denervation

Data from the denervation studies did not confirm the initial hypothesis that leptin would prevent IR induced by hindlimb denervation (Fig. 23). Several technical and methodological difficulties, including duration of virus treatment and denervation, contributed to the abandonment of this particular arm of the study. However, future studies using this model may be helpful in clarifying mechanisms associated with improved insulin sensitivity such as alteration in SkM lipid content and activation of membrane-associated PKCθ.

H. Final conclusions and limitations

In conclusion, it has been established that acute hyperlipidemia in the form of lipid infusion elicits IR. Mechanisms associated with the development of SkM IR include increases in SkM lipid species DAG and ceramide and the activation of membrane associated PKCθ leading to subsequent deleterious effects on the insulin-signaling cascade and decreases in insulin-stimulated glucose uptake (15, 24, 47, 59). The administration of leptin in the diet-induced obesity and genetic models of IR elicits a decrease in SkM lipids and subsequent improvements of insulin action (7, 11, 58). This study demonstrates that leptin treatment, in the form of adenovirus overexpression, prevents the development of SkM IR by acute lipid oversupply. Associated mechanisms include a prevention of accumulation in SkM lipid species (DAG and ceramide) and a decrease in the activation of membrane-associated PKCθ. The data suggest that other mechanisms including increased FAox and increased P-ACC, while potentially contributing to the observation, are not observed to be different following 5d of HLEP.

There are several limitations to the conclusions of this study. First, the method of leptin treatment, adenovirus, is a forced increase in circulating leptin levels. As such, it is unknown

if this approach elicits similar metabolic responses compared to normal-physiologic leptin levels. Second, as stated previously the analysis of differences between leptin and βGal treatments occurred at a set time-point (5d). Mechanisms associated with leptin prevention of IR (increased FAox, decreased FAT/CD36 and FABPpm, or increased P-ACC) may be detectable earlier in the treatment period, however after chronic HLEP, these enhancements may be missed. Finally, the current studies were conducted in the rat. It is recognized that there are differences in energy metabolism and thermogenesis between humans and rodents (38). However, animal studies do provide the framework for insights into human disease. Taken together these data demonstrate that leptin is an important modulator of insulin sensitivity. Moreover, leptin is able to prevent lipid induced IR in a non-obese model through prevention of accumulated lipid metabolites and decreased activation of membrane-associated PKCθ. Additional studies should be conducted to further characterize the time required for leptin to prevent lipid induced insulin resistance.

Literature Cited

1. **Adams, J. M. 2nd., T. Pratipanawatr, R. Berria, E. Wang, R.A. DeFronzo, M.C. Sullards, and L.J. Mandarino**. Ceramide content is increased in skeletal muscle from obese insulin-resistant humans. *Diabetes*. 53:25-31, 2004.

2. **Berg, J.P.** Leptin is a potent anti-diabetic in mice with lipodystrophy and insulin resistance. *European Journal of Endocrinology*. 142:114-116, 2000.

3. **Boden, G., F. Jadali, J. White, M. Mozzoli, X. Chen, E. Coleman, and C. Smith**. Effects of fat on insulin-stimulated carbohydrate metabolism in normal men. *J. Clin. Invest.* 88:960-966, 1991.

4. **Boden, G., X. Chen, J. Ruiz, J.V. White, and L. Rossetti**. Mechanisms of fatty acid-induced inhibition of glucose uptake. *J. Clin. Invest.* 93:2438-2446, 1994.

5. **Bonen, A., C.R. Benton, S.E. Campbell, A. Chabowski, D.C. Clarke, X.-X. Han, J.F.C. Glatz, and J.J.F.P. Luiken**. Plamalemmal fatty acid transport is regulated in heart amd skeletal muscle by contraction, insulin and leptin, and in obesity and diabetes. *Acta. Pyhsiol. Scand.* 178:347-356, 2003.

6. **Bonen, A., J.J.F.P. Luiken, S. Liu, D.J. Dyck, B. Kiens, S. Kristiansen, L.P. Turcotte, G.J. Van der Vusse, and J.F.C. Glatz**. Palmitate transport and fatty acid transporters in red and white muscles. *Am. J. Physiol. Endocrinol. Metab.* 275:E471-E478, 1998.

7. **Buettner, R., C.B. Newgard, C.J. Rhodes, and R.M. O'Doherty**. Correction of diet-induced hyperglycemia, hyperinsulinemia, and skeletal muscle insulin resistance by moderate hyperleptinemia. *Am. J. Physiol. Endocrinol. Metab.* 278:E563-E569, 2000.

8. **Castello, A., J. Cadefau, R. Cusso, X. Testar, J.E. Hesketh, M. Palacin, and A. Zorzano**. GLUT-4 and GLUT-1 glucose transporter expression is differentially regulated by contractile activity in skeletal muscle. *J. Biol. Chem.* 268:14998-15003, 1993.

9. **Chen, G., K. Koyama, X. Yuan, Y. Lee, Y.T. Zhou, R. O'Doherty, C.B. Newgard, and R.H. Unger**. Disappearance of body fat in normal rats induced by adenovirus-mediated leptin gene therapy. *Proc. Natl. Acad. Sci. USA*. 93:14795-14799, 1996.

10. **Chen, K.S., S.J. Heydrick, M.L. Brown, J.C. Friel, and N.B. Rudderman**. Insulin increases a biochemically distinct pool of diacylglycerol in the rat soleus muscle. *Am. J. Physiol. Endocrinol. Metab.* 266:E479-E485, 1994.

11. **Chinookoswong, N., J.L. Wang, and Z.Q. Shi**. Leptin restores euglycemia and normalizes glucose turnover in insulin-deficient diabetes in the rat. *Diabetes*. 48:1487-1492, 1999.

12. **Davis, T.A. and I.E. Karl.** Resistance of protein and glucose metabolism to insulin in denervated rat muscle. *Biochem. J.* 254:667-675, 1988.

13. **Diamond, J.** The double puzzle of diabetes. *Nature*. 423:599-602, 2003.

14. **Dobrzyn, A. and J. Gorski.** Ceramides and sphingomyelins in skeletal muscles of the rat: content and composition. Effect of prolongs exercise. *Am. J. Physiol. Endocrinol. Metab.* 281:E277-E285, 2002.

15. **Dresner, A., D. Laurent, M. Marcucci, M.E. Griffen, S. Dufour, G.W. Cline, L.A. Slezak, D.K. Anderson, R.S. Hundal, D.L. Rothman, K.F. Petersen, and G.I. Shulman**. Effects of free fatty acids on glucose transport and IRS-1-associated phosphatidylinositol 3-kinase activity. *J. Clin. Invest.* 103:253-259, 1999.

16. **Elbein, S.C.** Genetics of type 2 diabetes: an overview for the millennium. *Diabetes Technol Ther*. 2:391-400, 2000.

17. **Elmendorf, J.S., A. Damrau-Abney, T.R. Smith, T.S. David, and J. Turinsky**. Phosphatidylinositol 3-kinase and dynamics of insulin resistance in denervated slow and fast muscle in vivo. *Am. J. Physiol. Endocrinol. Metab.* 272:E661-E670, 1997.

18. **Fleber, J. and A. Golay.** Pathways from obesity to diabetes. *International Journal of Obesity*. 26:S39-S45, 2002.

19. **Folch, J., M. Lees, and G.H. Sloane Stanley**. A simple method for the isolation and purification of total lipides from animal tissues. *J. Biol. Chem.* 226:497-509, 1957.

20. **Goodpaster, B.H., and D.E. Kelley**. Skeletal muscle triglyceride: marker or mediator of obesity-induced insulin resistance in type 2 diabetes mellitus? *Curr. Diab. Rep*. 2:216-222, 2002.

21. **Goodpaster, B.H., D.E. Kelley, R.R. Wing, A. Meier, and F.L. Thaete**. Effects of weight loss on regional fat distribution and insulin sensitivity in obesity. *Diabetes*. 48:839-847, 1999.

22. **Goodpaster, B.H., J. He, S. Watkins, and D.E. Kelley**. Skeletal muscle lipid content and insulin resistance: evidence for a paradox in endurance-trained athletes. *J. Clin. Endocrinol. Metab.* 86:5755-5761, 2001.

23. **Gorski, J., A. Dobrzyn, and M. Zendzian-Piotrowska**. The sphingomyelin-signaling pathway in skeletal muscle and its role in regulation of glucose uptake. *Ann. N.Y. Acad. Sci.* 96:236-248, 2002.

24. **Griffin, M.E., M.J. Marcucci, G.W. Cline, K. Bell, N. Barucci, D. Lee, L.J. Goodyear, E.W. Kraegan, M.F. White, G.I Shulman**. Free fatty acid-induced insulin resistance is associated with activation of protein kinase C θ and alterations in the insulin signaling cascade. *Diabetes*. 48:1270-1274, 1999.

25. **Halaas, J.L., C. Boozer, J. Blair-West, N. Fidahusein, D.A. Denton, and J.M. Friedman**. Physiological responce to long-term peripheral and central leptin infusion in lean and obese mice. *Proc. Natl. Acad. Sci. USA*. 94:8878-8883, 1997.

26. **Halaas, J.L., K.S. Gajiwala, M. Maffei, S.L. Cohen, B.T. Chait, D. Rabinowitz, R.L. Lallone, S.K. Burley, and J.M. Friedman**. Weight-reducing effects of the plasma protein encoded by the obese gene. *Science*. 269:543-546, 1995.

27. **Hegarty, B.D., S.M. Furler, J. Ye, G.J. Cooney, and E.W. Kraegen**. The role of intramusclar lipid in insulin resistance. *Acta. Pyhsiol. Scand.* 178:373-383, 2003.

28. **Hervey, G.R.** The effects of lesions in the hypothalamus in parabiotic rats. *J. Physiol.* 145:336-352, 1959.

29. **Heydrick, S.J., N.B. Ruderman, T.G. Kurowski, H.B. Adams, and K.S. Chen**. Enhanced stimulation of diacylglycerol and lipid synthesis by insulin in denervated muscle. Altered protein kinase C activity and possible link to insulin resistance. *Diabetes*. 40:1707-1711, 1991.

30. **Hung, T., J.L. Sievenpiper, A. Marchie, C.W.C. Kendall, and D.J.A. Jenkins**. Fat versus carbohydrate in insulin resistance, obesity, diabetes and cardiovascular disease. *Curr. Opin. Clin. Nutr. Metab. Care*. 6:165-176, 2003.

31. **Itani, S.I., N.B. Rudderman, F. Schmieder, and G. Boden**. Lipid-induced insulin resistance in human muscle is associated with changes in diacylglycerol, protein kinase C and IκB-α. *Diabetes*. 51:2005-2011, 2002.

32. **Kelley, D.E., and J.A. Simoneau**. Impaired free fatty acid utilization by skeletal muscle in non-insulin-dependent diabetes mellitus. *J. Clin. Invest.* 94:2349-2356, 1994.

33. **Kim, J.K., J.J. Filmore, M.J. Sunshine, B. Albrecht, T. Higashimori, D. Kim, Z. Liu, T.J. Soos, G.W. Cline, W.R. O'Brien, D.R. Littman, and G.I. Shulman**. PKCθ knockout mice are protected from fat-induced insulin resistance. *J. Clin. Invest.* 114:823-827, 2004.

34. **Kim, J.K., J.K. Wi, and J.H. Youn**. Metabolic impairment precedes insulin resistance in skeletal muscle during high-fat feeding in rats. *Diabetes*. 45:651-658, 1996.

35. **Kim, Y.-B., G.I. Shulman, and B.B. Kahn**. Fatty acid infusion selectively impairs insulin action on Akt1 and protein kinase C λ/ζ but not on glycogen synthase kinase-3. *J. Biol. Chem.* 277:32915-32922, 2002.

36. **Muoio, D.M., G.L. Dohm, E.B. Tapscott, and R.A. Coleman**. Leptin opposes insulin's effects on fatty acid partitioning in muscles isolated from obese *ob/ob* mice. *Am. J. Physiol. Endocrinol. Metab.* 276:E913-E921, 1999.

37. **Muoio, D.M., G.L. Dohm, F.T. Fiedorek, E.B. Tapscott, and R.A. Coleman**. Leptin directly alters lipid partitioning in skeletal muscle. *Diabetes*. 46:1360-1363, 1997.

38. **Muoio, D.M. and G.L. Dohm.** Peripheral metabolic actions of leptin. *Best Practice & Research Clinical Endocrinology and Metabolism*. 16:653-666, 2002.

39. **Muzzin, P., R.C. Eisensmith, K.C. Copeland, and S.L. Woo**. Correction of obesity and diabetes in genetically obese mice by leptin gene therapy. *Proc. Natl. Acad. Sci. USA*. 93:14804-14808, 1996.

40. **Oakes, N.D., G.J. Cooney, S. Camilleri, D.J. Chisholm, and E.W. Kraegen**. Mechanisms of liver and muscle insulin resistance induced by chronic high-fat feeding. *Diabetes*. 46:1768-1774, 1997.

41. **Oakes, N.D., K.S. Bell, S.M. Furler, S. Camilleri, A.K. Saha, N.B. Rudderman, D.J. Chisholm, and E.W. Kraegen**. Diet-induced muscle insulin resistance in rats is ameliorated by acute dietary lipid withdrawal or a single bout of exercise: parallel relationship between insulin stimulation of glucose uptake and suppression of long-chain fatty acyl-CoA. *Diabetes*. 46:2022-2028, 1997.

42. **Petersen, K.F., E. A. Oral, S. Dufour, D. Befroy, C. Ariyan, C. Yu, G.W. Cline, A.M. DePaoli, S.I. Taylor, P. Gorden, and G.I. Shulman**. Leptin reverses insulin resistance and hepatic steatosis in patients with severe lipodystrophy. *J. Clin. Invest.* 109:1345-1350, 2002.

43. **Preiss, J., C.R. Loomis, W.R. Bishop, R. Stein, J.E. Niedel, and R.M. Bell**. Quantitative measurement of sn-1,2-diacylglycerols present in platelets, hepatocytes, and ras- and sis-transformed normal rat kidney cells. *J. Biol. Chem.* 261:8597-8600, 1986.

44. **Roden, M., T.B. Price, G. Perseghin, K.F. Petersen, D.L. Rothman, G.W. Cline, and G.I. Shulman**. Mechanism of free fatty acid-induced insulin resistance in humans. *J. Clin. Invest.* 97:2859-2865, 1996.

45. **Roepstorff, C., J.W. Helge, B. Vistisen, and B. Kiens**. Studies of plasma membrane fatty acid-binding proteins in human skeletal muscle. *Proceedings of the Nutritional Society*. 63:239-244, 2004.

46. **Romijn, J.A., E.F. Coyle, L.S. Sidossis, A. Gastaldelli, J.F. Horowitz, E. Endert, and R.R. Wolfe**. Regulation of endogenous fat and carbohydrate metabolism in relation to exercise intensity and duration. *Am. J. Physiol. Endocrinol. Metab.* 265:E380-E391, 1993.

47. **Schmitz-Peiffer, C.** Signalling aspects of insulin resistance in skeletal muscle: mechanisms induced by lipid oversupply. *Cellular Signaling*. 12:583-594, 2000.

48. **Schmitz-Peiffer, C., D.L. Craig, T.J. and Biden**. Ceramide generation is sufficient to account for the inhibition of the insulin-stimulated PKB pathway in C2C12 skeletal muscle cells pretreated with palmitate. *J. Biol. Chem.* 274:24202-24210, 1999.

49. **Smith, R.L., P.J. Roach, and J.C. Lawrence**. Insulin resistance in denervated skeletal muscle. *J. Biol. Chem.* 263:658-665, 1988.

50. **Solinas, G., S. Summermatter, D. Mainieri, M. Gubler, L. Pirola, M.P. Wymann, S. Rusconi, J. Montani, J. Seydoux, and A.G. Dulloo**. The direct effect of leptin on skeletal muscle thermogenesis is mediated by substrate cycling between de novo lipogenesis and lipid oxidation. *FEBS Letters*. 577:539-544, 2004.

51. **Steinberg, G.R., D.J. Dyck, J. Calles-Escandon, N.N. Tandon, J.J.F.P. Luiken, J.F.C. Glatz and A. Bonen**. Chronic leptin administration decreases fatty acid uptake and fatty acid transporters in rat skeletal muscle. *J. Biol. Chem.* 277:8854-8860, 2002.

52. **Steinberg, G.R., A. Bonen, and D.J. Dyck**. Fatty acid oxidation and triacyglycerol hydrolysis are enhanced after chronic leptin treatment in rats. *Am. J. Physiol. Endocrinol. Metab.* 282:E593-E600, 2002.

53. **Stratford, S., K.L. Hoehn, F. Liu, S.A. Summers**. Regulation of insulin action by ceramide. *J. Biol. Chem.* 279:36608-36615, 2004.

54. **Surwit, R.S., C.L. Edwards, S. Murthy, and A.E. Petro**. Transient effects of long-term leptin supplementation in the prevention of diet-induced obesity in mice. *Diabetes*. 49:1203-1208, 2000.

55. **Turinsky, J., D.M. O'Sullivan, and B.P. Bayly**. 1,2-Diacylglycerol and ceramide levels in insulin-resistant tissues of the rat *in vivo*. *J. Biol. Chem.* 265:16880-16885, 1990.

56. **Turinsky, J. and A. Damrau-Abney.** Akt1 kinase and dynamics of insulin resistance in denervated muscles in vivo. *Am. J. Physiol. Regulatory Integrative Comp. Physiol.* 275:R1425-R1430, 1998.

57. **Vettor, R., R. Fabris, R. Sarra, A.M. Lombardi, C. Tonello, M. Granzotto, M.O. Marzolo, M.O. Carruba, D. Ricqueir, G. Federspil, and E. Nisoli**. Changes in FAT/CD36, UCP2, UCP3 and GLUT4 gene expression during lipid infusion in rat skeletal and heart muscle. *International Journal of Obesity*. 26:838-847, 2002.

58. **Yaspelkis, B.B., M. Saberi, M.K. Singh, B. Trevino, and T.L. Smith**. Chronic leptin treatment normalizes basal glucose transport in a fiber type-specific manner in high-fat-fed rats. *Metabolism*. 51:859-863, 2002.

59. **Yu, C., G.W. Cline, D. Zhang, H. Zong, Y. Wang, R. Bergeron, J.K. Kim, S.W. Cushman, G.J. Cooney, B. Atcheson, M.F. White, E.W. Kraegen, and G.I. Shulman**. Mechanism by which fatty acids inhibit insulin activation of insulin receptor substrate-1 (IRS-1)-associated phosphatidylinositol 3-kinase activity in muscle. *J. Biol. Chem.* 277:50230-50236, 2002.

60. **Zernicka, E.E.S., J. Langfort, and M. Gorecka**. Time course of changes in lipoprotein lipase activity in rat skeletal muscles during denervation-reinnervation. *J. Appl. Physiol.* 92:535-540, 2002.